SLAC-PUB-15061

Prepared for submission to JCAP

Dark matter searches with Cherenkov telescopes: nearby dwarf galaxies or local galaxy clusters?

Miguel A. Sánchez-Conde,[a,b,c] **Mirco Cannoni,**[d] **Fabio Zandanel,**[e] **Mario E. Gómez**[d] **and Francisco Prada**[e]

[a]SLAC National Laboratory and Kavli Institute for Particle Astrophysics and Cosmology, 2575 Sand Hill Road, Menlo Park, CA 94025, USA

[b]Instituto de Astrofisica de Canarias, E-38205 La Laguna, Tenerife, Spain

[c]Dpto. Astrofísica, Universidad de La Laguna (ULL), E-38205 La Laguna, Tenerife, Spain

[d]Dpto. Física Aplicada, Facultad de Ciencias Experimentales, Universidad de Huelva, 21071 Huelva, Spain

[e]Instituto de Astrofísica de Andalucía (CSIC), E-18008, Granada, Spain

Abstract. In this paper, we compare dwarf galaxies and galaxy clusters in order to elucidate which object class is the best target for gamma-ray DM searches with imaging atmospheric Cherenkov telescopes (IACTs). We have built a mixed dwarfs+clusters sample containing some of the most promising nearby dwarf galaxies (Draco, Ursa Minor, Wilman 1 and Segue 1) and local galaxy clusters (Perseus, Coma, Ophiuchus, Virgo, Fornax, NGC 5813 and NGC 5846), and then compute their DM annihilation flux profiles by making use of the latest modeling of their DM density profiles. We also include in our calculations the effect of DM substructure. Willman 1 appears as the best candidate in the sample. However, its mass modeling is still rather uncertain, so probably other candidates with less uncertainties and quite similar fluxes, namely Ursa Minor and Segue 1, might be better options. As for galaxy clusters, Virgo represents the one with the highest flux. However, its large spatial extension can be a serious handicap for IACT observations and posterior data analysis. Yet, other local galaxy cluster candidates with more moderate emission regions, such as Perseus, may represent good alternatives. After comparing dwarfs and clusters, we found that the former exhibit annihilation flux profiles that, at the center, are roughly one order of magnitude higher than those of clusters, although galaxy clusters can yield similar, or even higher, integrated fluxes for the whole object once substructure is taken into account. Even when any of these objects are strictly point-like according to the properties of their annihilation signals, we conclude that dwarf galaxies are best suited for observational strategies based on the search of point-like sources, while galaxy clusters represent best targets for analyses that can deal with rather extended emissions. Finally, we study the detection prospects for present and future IACTs in the framework of the constrained minimal supersymmetric standard model. We find that the level of the annihilation flux from these targets is below the sensitivities of current IACTs and the future CTA.

Keywords: Dark matter, supersymmetry, dwarf galaxies, cluster of galaxies, gamma rays, Cherenkov telescopes

ArXiv ePrint: 1104.3530

Work supported in part by US Department of Energy contract DE-AC02-76SF00515.

Contents

1 Introduction **1**

2 Flux of gamma rays from DM annihilation **3**
2.1 $J(\Psi_0)$: the astrophysical flux factor 4
2.1.1 Reference values of the astrophysical factor 5
2.2 The particle physics factor, f_{SUSY}, in CMSSM 6

3 DM searches in dwarf galaxies **8**
3.1 Selection of the sample 8
3.2 Looking for the best candidate 9

4 DM searches in galaxy clusters **13**
4.1 The selection of our sample 13
4.2 Looking for the best candidate 14
4.3 The effect of substructure 15
4.4 γ-rays with a non-DM origin in clusters 18

5 DM annihilation flux predictions and detection prospects for IACTs **19**
5.1 Galaxy clusters or dwarf galaxies? 19
5.2 J-values comparison with other works 20
5.3 Milky Way foreground 22
5.4 Flux predictions 23

6 Summary and conclusions **25**

1 Introduction

During the last century, many astrophysical observations on different scales seemed to point to the fact that the luminous matter in the Universe is just a tiny fraction of its total content. Effectively, there exists strong evidence for believing that most of the matter in our Universe is dark. This dark matter (DM) has not been directly detected in the laboratory yet, but its gravitational effects have been observed on all spatial scales, from the inner kiloparsecs of galaxies out to Mpc and cosmological scales. One of the first steps in the DM paradigm was taken by F. Zwicky in the 1930s to explain the velocity dispersion in galaxy clusters. Today, the most conclusive observations in this sense come from the rotational speeds of galaxies, the orbital velocities of galaxies within clusters, gravitational lensing, satellite kinematics, the cosmic microwave background, the light element abundances and large scale structure [1].

However, we still do not know what the DM is made of. Physics beyond the Standard Model of Particle Physics needs to be invoked, where good non-baryonic DM candidates arise to fulfill all the cosmological requirements. In the Lambda Cold Dark Matter (ΛCDM) paradigm, around 23% of the Universe consists of non-baryonic DM [2]. A plethora of possible DM candidates have already been proposed. Axion-like particles, proposed for different reasons in an extension of the Standard Model of particle physics, represent one of the most

popular candidates [3, 4]. Ordinary massive neutrinos are too light to be cosmologically significant, though sterile neutrinos remain a possibility. Other candidates include primordial black holes, non-thermal WIMPzillas, and Kaluza-Klein particles (see Refs. [5, 6] for a recent and detailed picture). The neutralino is probably the most studied candidate and it arises in supersymmetric (SUSY) extension of the Standard Model of particle physics. In particular, in the minimal supersymmetric standard model (MSSM) R-parity is conserved and the the lightest SUSY particle is one of the neutralinos, which is a stable Majorana particle with a relic density compatible with WMAP bounds. In this work we consider the lightest neutralino to be the DM particle. Being the neutralino its own antiparticle, it annihilates when interacting with other neutralinos. This fact is crucial for detectability purposes, as one of the products of these annihilations are predicted to be gamma-rays, whose specific energy will vary according to the chosen particle physics model, but that is expected to lie in the energy range covered by the current imaging atmospheric Cherenkov telescopes (IACTs). The imaging atmospheric Cherenkov technique, first pioneered by the Whipple collaboration, currently leads above 100 GeV by HESS [7], MAGIC [8] and VERITAS [9]. Also the NASA Fermi satellite [10] is playing a major role in the exploration of the gamma-ray energy regime, namely between 20 MeV up to ∼300 GeV. This study, however, will mainly focus on DM searches with IACTs.

The DM annihilation flux is proportional to the annihilation rate, which is proportional to the squared DM density. This means that the best places to look for DM will be those with the highest DM concentrations. Distance is also very important, since highly DM-dominated systems that are located too far from us will yield too low DM annihilation fluxes at Earth. Keeping both considerations in mind, IACT efforts have focused on the Galactic Center [11–13] and dwarf galaxy satellites of the Milky Way [14, 15]. Nearby galaxy clusters may also represent very suitable targets, given their large DM content; indeed, they may yield similar gamma-ray fluxes despite their distance (see e.g. [16]). At present, many of these objects have already been observed in γ-rays. Unfortunately, no clear signal from DM annihilation has been found yet (at least unequivocally; for example, see [17] for some hints of detection). In the last few years, most attention have been devoted to the search for neutralino annihilations in nearby dwarf galaxies [18–25] rather than in massive nearby galaxy clusters, although up to now no one has studied in detail which kind of object class would be preferable for DM searches.

The main aim of this study is to compare both the expected DM annihilation fluxes from the most promising dwarfs and galaxy clusters in order to elucidate which object class is most suitable for gamma-ray DM searches with present and future IACTs. We make use of the latest modeling of DM density profiles calculated from the latest available observational data. We also carefully include the effect of DM substructure, taking as reference the procedure described in Ref. [26]. On the particle physics side, we do include internal bremsstrahlung in the computation of the number of photons per annihilation (see, for example, [27]). This effect might significantly enhance the DM annihilation flux for specific models of the allowed parameter space [28]. We do not consider, however, models with Sommerfeld enhancement, which may provide an additional boost to the flux [29][1].

[1]This effect depends on the mass of the DM particle and its velocity, which means that it is necessary to know in detail the velocity distribution of the DM particles inside the objects. This is beyond the scope of this paper. Furthermore, the importance of the Sommerfeld effect is very sensible to e.g. little variations of the considered DM particle mass or other slight changes in the involved parameters (as shown e.g. in Ref. [30]). Therefore, we decided not to include this effect and to keep conservative in deriving our detection limits. In

We furthermore perform a detailed analysis of the expected gamma-ray DM annihilation flux from each object by defining and calculating some specific quantities that were carefully chosen taking into account both the instrumental and observational properties of IACTs. These new parameters will contribute with relevant information to our understanding of the particular characteristics that a gamma-ray flux with a DM-annihilating origin may necessarily exhibit. We select our sample according to i) previous estimates of the DM annihilation flux, ii) distance, iii) an acceptable knowledge of the DM content, and iv) abundant literature. With all these considerations in mind, we finally focused our efforts on four dwarf galaxy satellites of the Milky Way (Draco, Ursa Minor, Willman 1, and Segue 1), and seven galaxy clusters (Perseus, Coma, Ophiuchus, Virgo, Fornax, NGC 5813, and NGC 5846). We refer the reader to sections 3 and 4 respectively for further details on the sample selection.

This article is organized as follows. In section 2 we discuss the factors involved in the computation of the gamma-ray DM annihilation flux: the astrophysical factor in section 2.1 (with the definition of some reference values in 2.1.1), and the particle physics factor in 2.2. In section 3 we perform a detailed study of the DM annihilation flux for our sample of dwarf galaxies, discussing the best observational strategies to be followed for a successful search. A similar strategy is followed for galaxy clusters in section 4, this time including substructure as well. We finally compare the DM annihilation prospects for dwarfs and clusters in section 5 and state our conclusions in section 6.

2 Flux of gamma rays from DM annihilation

Why γ-rays and not other wavelengths? The key point is the energy scale of the annihilation products, which is determined by the mass of the DM particles. Since preferred DM candidates like the neutralino are expected to have masses in the ∼GeV–TeV range[2], DM searches are specially performed in the γ-ray energy band. However, we stress that multi-wavelength studies could be of considerable importance in constraining DM models and therefore should also be taken into account in order to reach a consistent general picture (e.g., Refs. [35–37]).

In this study we will make the assumption that the neutralino χ is the main component of the DM[3]. The expected total number of continuum γ-ray photons received per unit time and per unit area, above the energy threshold E_{th} of the telescope, when observing at a given direction Ψ_0 relative to the centre of the DM halo is given by:

$$F(E_\gamma > E_{\rm th}, \Psi_0) = J(\Psi_0) \times f_{SUSY}(E_\gamma > E_{\rm th}). \tag{2.1}$$

The factor f_{SUSY} incorporates all the particle physics, whereas all the astrophysical considerations are included in $J(\Psi_0)$. We discuss both factors in the next two subsections.

any case, we note that according to recent estimates, Sommerfeld enhancements are not probably larger than ∼5 for clusters [31].

[2] The evidence of an annual modulation in the rate of elastic WIMP-nucleus scattering claimed by DAMA [32] and recently by CoGENT [33] favours a light WIMP with mass around 10 GeV that is not an ideal candidate for gamma ray detection with IACT. The results of other experiments are in contrast with this conclusion, thus at present there is no clear indication in favour or against a light WIMP [34].

[3] Note that the total amount of DM in the Universe could not be constituted by a single class of DM particle. Indeed, we already know that standard neutrinos contribute to DM, although they cannot account for all of it. A discussion on the detection prospects of a sub-dominant density component of DM can be found, for example, in [38].

2.1 $J(\Psi_0)$: the astrophysical flux factor

$J(\Psi_0)$ in eq.(2.1) accounts for the DM distribution, the geometry of the problem, and also the instrumental effects induced by the IACT; i.e.,

$$J(\Psi_0) = \frac{1}{4\pi} \int U(\Psi_0) B(\Omega) d\Omega, \tag{2.2}$$

where $B(\Omega)d\Omega$ represents the beam smearing of the telescope, commonly known as the point spread function (PSF). The PSF can be well approximated by a Gaussian:

$$B(\Omega)d\Omega = \frac{1}{\sqrt{2\pi\sigma_t^2}} \exp\left[-\frac{\theta^2}{2\sigma_t^2}\right] \sin\theta \; d\theta \; d\phi, \tag{2.3}$$

with σ_t the angular resolution of the IACT. The $U(\Psi_0)$ factor of eq.(2.2) represents the integral of the line of sight (l.o.s.) of the DM density squared along the direction of observation Ψ_0:

$$U(\Psi_0) = \int_{l.o.s.} \rho_{DM}^2(r) \; d\lambda = \int_{\lambda_{min}}^{\lambda_{max}} \rho_{DM}^2[r(\lambda)] \; d\lambda. \tag{2.4}$$

Here, ρ_{DM} is the DM density profile and r represents the galactocentric distance, related to the distance λ to the Earth by:

$$r = \sqrt{\lambda^2 + R_\odot^2 - 2 \; \lambda \; R_\odot \cos\Psi}, \tag{2.5}$$

where $R_\odot$ is the distance from the Earth to the centre of the halo, and Ψ is related to the angles Ψ_0, θ and ϕ by the relation $\cos\Psi = \cos\Psi_0 \cos\theta + \sin\Psi_0 \sin\theta \cos\phi$. The lower and upper limits λ_{min} and λ_{max} in the l.o.s. integration are given by $R_\odot \cos\Psi \pm \sqrt{r_t^2 - R_\odot^2 \sin^2\Psi}$, where r_t is the radius of the object under consideration (e.g., the tidal radius in case of dwarfs).

One crucial aspect in the calculation of the astrophysical factor concerns the modeling of the DM distribution. Current N-body cosmological simulations suggest the existence of a universal DM density profile, with the same shape for all masses and epochs [39]. In Ref. [40], authors proposed a general parameterization for the DM halo density in order to agglutinate most of the fitting formulae that can be found in the literature:

$$\rho(r) = \frac{\rho_0}{\left(\frac{r}{r_s}\right)^\gamma \left[1 + \left(\frac{r}{r_s}\right)^\alpha\right]^{\frac{\beta-\gamma}{\alpha}}}, \tag{2.6}$$

where ρ_0 and r_s represent a characteristic density and a scale radius respectively. The Navarro-Frenk-White (hereafter NFW), with (α,β,γ) = (1,3,1), is by far the most widely DM density profile used in the literature [41]. Other studies seem to point to inner slopes of 1.2 [42]. Recently, also the so-called Einasto DM density profile is often used, motivated by the fact that state-of-the-art N-body cosmological simulations [43, 44] seem to point to a less steep DM density profile in the central regions of CDM halos, which in addition shows better agreement with observations [45–47]:

$$\rho(r) = \rho_s \exp\left[\frac{-2}{\alpha} \left(\left(\frac{r}{r_s}\right)^\alpha - 1\right)\right]. \tag{2.7}$$

The main controversy between different groups pertains to the slope of this profile in the innermost regions of galaxies and galaxy clusters, which are obviously the most conflictive regions to be simulated correctly. Uncertainties arise also from the effects of the adiabatic baryonic compression of the DM near the halo center [48], typically not considered in N-body simulations, as well as from the possible effect of central black holes (e.g., [49, 50]).

The PSF of the telescope, on the other hand, plays a crucial role in the correct interpretation of the observational data [51]. The present generation of IACTs have PSF$\sim$0.1° (i.e., σ_t=0.1° in eq.(2.3)), which means that any gamma source with an extension smaller than this value will appear as point-like to the telescope. For our purposes, it is important to understand that point-like, rather than extended, sources are more readily observable by IACTs[4]. This is particularly true for single telescopes, for which stereoscopic analysis is not possible. However, the DM gamma signal is expected to be extended, since it follows the DM distribution; hence it is clear that a good DM-oriented observational strategy should be able to find a compromise between these crucial instrumental/observational aspects and the peculiarities of the DM gamma emission in the most interesting astrophysical targets.

2.1.1 Reference values of the astrophysical factor

We will now define some quantities that will become extremely helpful throughout the rest of the paper.

J_T is the total astrophysical factor obtained integrating over the total angular extension of the object:

$$\mathrm{J}_T = \frac{1}{4\pi D^2} \int_V \rho^2_{DM}(r)\ dV, \tag{2.8}$$

D being the distance from the Earth to the center of the DM halo and r the galactocentric distance inside it. Note that this expression no longer depends on the PSF.

Quantities related to the *observed* (i.e., taking into account the PSF) flux profile up to a specific radius/angle are calculated with:

$$\mathrm{J}_{\psi'} = \frac{1}{4\pi} \times 2\pi \times \int_0^{\psi'} J(\Psi_0)\ \sin(\Psi_0)\ d\Psi_0 \tag{2.9}$$

where $J(\Psi_0)$ is given by eq. (2.2). In particular:

- $\psi' = \psi_{90}$ and r_{90} are, respectively, the angle and the radius that identify the region from which 90% of the gamma emission is expected to come. J_{90} indicates the corresponding astrophysical factor.
- $\psi' = 0.1°$ and r_{01} refers to the inner 0.1° of the halo, and J_{01} is the corresponding astrophysical factor.
- $\psi' = \psi_{r_s}$ is the angle subtended by the scale radius r_s, and J_{r_s} is the astrophysical factor associated to the region inside r_s;
- We further define $Rank_{01}$ and $Rank_{90}$ which order the candidates according to the values of J_{01} and J_{90}, respectively.

[4]IACT sensitivity is approximately linearly proportional to the source extension. This means that the detectability of a gamma-ray source is proportional to its luminosity divided by its size. This fact clearly makes point-like sources easier targets for IACTs.

We chose quantities related to 90% of the annihilation flux because this is typically the fraction of the total flux that comes from the region within r_s for an NFW profile. Therefore, it is probably better to plan observational strategies focused on detecting the flux from this smaller area rather than from the total extension of the source[5]. Furthermore, point-like sources are more readily observable by present IACTs, as already discussed above. This information is codified in J_{01} and r_{01}, which were specially selected by comparison with the typical IACT PSF $\sim 0.1^\circ$. In particular, the larger values of J_{01}/J_T give more point-like objects that are more easily detected.

2.2 The particle physics factor, f_{SUSY}, in CMSSM

As already pointed out, we consider R-parity conserving SUSY models such that the LSP, the lightest neutralino, is the main dark matter component. The mechanisms producing photons in neutralino annihilation are well known. The dominant contribution is typically constituted by *secondary photons* coming from the hadronisation and decay of the annihilation products [54]. The energy spectrum is continuous and decreasing towards m_χ. At the one loop level neutralinos annihilate into photons through the processes [55] $\chi\chi \to \gamma\gamma$ and $\chi\chi \to Z\gamma$. Outgoing photons are almost monochromatic (*lines*) with energies $E_\gamma \sim m_\chi$ and $E_\gamma \sim m_\chi - m_Z^2/4m_\chi$, respectively. Although these gammas would give a very clear signal, the cross section is $\mathcal{O}(\alpha^4)$, thus very small. Finally, *internal bremsstrahlung* (IB) [27] which consists on the emission of additional photons from neutralino pair annihilation into charged particles: $\chi\chi \to X\bar{X}\gamma$, X being a charged lepton or a W boson. The cross section is $\mathcal{O}(\alpha^3)$, thus in principle its contribution is between the tree-level secondaries and the loop-level monochromatic lines. However, its relevance strongly depends on the SUSY spectrum [28]. f_{SUSY} is thus given by:

$$f_{SUSY} = f_{cont} + f_{lines}, \tag{2.10}$$

$$f_{cont} = \left(\sum_f \int_{E_{th}}^{m_\chi} \frac{dN_\gamma^f}{dE_\gamma} dE_\gamma \right) \frac{\langle \sigma_{\chi\chi}\, v \rangle}{2m_\chi^2} = f_{sec} + f_{IB}, \tag{2.11}$$

$$f_{lines} = 2\frac{\langle \sigma_{\gamma\gamma}\, v \rangle}{2m_\chi^2} + \frac{\langle \sigma_{Z\gamma}\, v \rangle}{2m_\chi^2}. \tag{2.12}$$

dN_γ^f/dE_γ is the differential yield of photons per annihilation to the final state f, thus $n_\gamma(E_\gamma > E_{th})$ is the total number of photons per annihilation with energy greater than the threshold energy. $\langle \sigma_{\chi\chi}\, v \rangle$ is the thermal averaged total neutralino annihilation cross section, $\langle \sigma_{\gamma\gamma}\, v \rangle$ and $\langle \sigma_{Z\gamma}\, v \rangle$ the cross sections for annihilation into lines and m_χ the neutralino mass.

The soft potential of the general MSSM at the weak scale contains more than a hundred free parameters: this large number is drastically reduced by adding further theoretical assumptions at the energy scale where the gauge couplings constants of the standard model unify (GUT scale). The benchmark theory with a low number of free parameters, which is the subject of the majority of phenomenological studies, is the constrained minimal supersymmetric standard model (CMSSM) [52]. The theory at the weak scale is determined by four parameters: the common scalar mass m_0, the common gauginos mass $m_{1/2}$, the common trilinear couplings A_0 assigned at the GUT scale, and the ratio of the Higgs vacuum expectation values, $\tan\beta$. The sign of μ, the Higgs mixing term, is left undetermined: we consider

[5] In the latter case, we will be introducing a lot of extra background without significantly increasing the annihilation signal. In dwarfs, for instance, r_s typically represents less than 10% of the total radius.

Model	$\tan\beta$	m_0 (GeV)	$m_{1/2}$ (GeV)	A_0 (GeV)	$m_{\tilde{\chi}}$ (GeV)	$\Omega_\chi h^2$	$\langle\sigma_{\chi\chi}v\rangle$ ($\mathrm{cm}^3\ \mathrm{s}^{-1}$)	f_{SUSY} ($\mathrm{GeV}^{-2}\mathrm{cm}^3\mathrm{s}^{-1}$)
A	18	127	459	−135	187.6	0.092	0.03×10^{-26}	0.1×10^{-32}
B	52	982	1377	725	597.6	0.092	2.6×10^{-26}	0.72×10^{-32}
C	17	2200	430	805	162.8	0.098	2.2×10^{-26}	0.12×10^{-32}
D	51	8940	2218	−4221	918.2	0.099	1.2×10^{-26}	0.32×10^{-32}

Table 1. Reference models in the CMSSM with $\mu > 0$ and the corresponding relevant physical quantities for γ-ray production and detection. The value of the particle physics factor f_{SUSY} is obtained integrating on photon energies above the threshold $E_{th} = 100$ GeV.

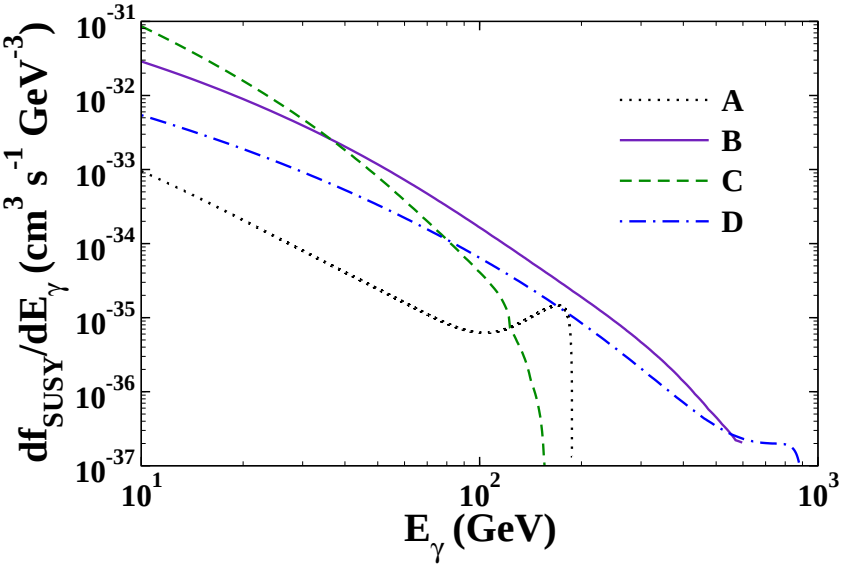

Figure 1. Differential particle physics factor as a function of γ-ray energy for the models reported in table 1. See text for further details and discussion.

in the following the case $\mu > 0$. We select SUSY models such that the relic abundance of the neutralino is inside the cosmologically favoured WMAP interval [53], $0.09 < \Omega_\chi h^2 < 0.13$ at 3σ. In addition we impose the LEP bounds on the masses of the light Higgs and the chargino, $m_h > 114$ GeV and $m_{\chi^+} > 103.5$ GeV [6], and the constraints from $b \to s\gamma$.

For fixed values of $\tan\beta$ and A_0, only narrow regions of the CMSSM parameter space in the ($m_{1/2}$, m_0) plane pass the phenomenological constraints: 1) the stau coannihilation region where the next lightest SUSY particle, the scalar partner of the tau fermion, is nearly degenerate in mass with the lightest neutralino; 2) the Higgs funnel region where the neutralino mass is nearly half of the pseudo-scalar Higgs boson A; 3) the focus-point region at large m_0 where the neutralino has a large higgsino component.

In table 1 we provide some reference models chosen from an exhaustive scan of the CMSSM parameter space in Ref. [28]. Model A is in the stau coannihilation region, Model B is in the funnel region and Models C and D are in the focus point region. The numerical values for the neutralino mass, the relic density, the total annihilation cross section and

[6] In the CMSSM and other SUSY models with gaugino mass unification, the mass of the charginos and the mass of the neutralinos are strictly correlated. The bound on the lightest chargino mass does not allow for a light neutralino with mass below $\simeq 50$ GeV.

f_{SUSY} with $E_{th} = 100$ GeV were obtained using the code DarkSusy 5.0.5 [57].

The most optimistic value of f_{SUSY}, with a typical IACT threshold energy $E_{th} = 100$ GeV, is $\simeq 10^{-32}$ GeV^{-2} cm^3 s^{-1} and it is found in Model B. As explained above, in this case $m_A \simeq 2m_\chi$. The large annihilation cross section is determined by the diagram with s-channel resonant pseudo-scalar Higgs boson propagator. The branching ratios of the final states from A decay are $\sim 87\%$ in $b\bar{b}$ and $\sim 13\%$ in $\tau^+\tau^-$ that result in a large amount of gamma in the subsequent hadronization.

Model C and D predict values of f_{SUSY} of the same order of magnitude but smaller than Model B. In these cases the main annihilation final states are W^+W^- and ZZ due to the larger higgsinos component in the neutralino that enhances the coupling to the gauge bosons.

In Model A the only relevant final states are $b\bar{b}$ and $\tau^+\tau^-$ (both with fraction around 50%) and the neutralino is bino-like as in Model B. In this case the resonant condition $m_A \simeq 2m_\chi$ is not satisfied thus the cross section, as can be seen in table 1, is two orders of magnitude smaller. In this model, on the other hand, the mass of the lightest stau is close to the neutralino mass, $m_{\tilde{\tau}} \gtrsim m_\chi$. The diagram with t-channel stau exchange, hence, is not suppressed with respect to diagrams with Higgs boson s-channel exchange. Furthermore, due to this mass degeneracy, the diagram with a photon line attached to t-channel stau propagator enhances the cross section at energies near the neutralino mass. The effect of IB is seen in the dotted line of figure 1 where we plot the df_{SUSY}/dE_γ as a function of E_γ: with the "bump" at energies near the neutralino mass, f_{SUSY} can be of the same order of magnitude as the other models, in any case remaining 1–2 orders of magnitude smaller at lower energies.

We will use Model B as a reference in section 5 where we discuss the predictions for the total fluxes because it provides the most optimistic scenario for detection.

3 DM searches in dwarf galaxies

3.1 Selection of the sample

Dwarf spheroidal (dSphs) satellites of the Milky Way are very good candidates for DM searches, as they are the most DM-dominated systems known in the Universe (with inferred mass-to-light (M/L) ratios as high as 1000 for some of the recently discovered dSphs) and are relatively close to us (less than 100 kpc in the case of Draco, UMi, and some of the new SDSS dwarfs). Moreover, most of them are expected to be free from bright astrophysical gamma sources, in contrast with other targets like the Galactic Center, nearby spiral galaxies, or very massive galaxy clusters.

Nowadays, we know the existence of at least 23 Milky Way satellites, more than half of them discovered in the last few years using SDSS data [58]. Most of them have typically higher M/L ratios and are closer than the previously well-known dwarfs. Both facts should increase the chance of DM detection. Nevertheless, observational data are still very scarce for most of them, so these numbers should be treated cautiously. A good example is Segue 1, which was catalogued as a unusually extended globular cluster soon after its discovery [59], later as a new ultra-faint dwarf galaxy [60, 61], then again as a globular cluster [62], and recently new studies were published that favors the scenario of a highly DM-dominated dwarf galaxy [63, 64]. The same might still happen to other similar objects such as Willman 1. At present, the latest word on Willman 1 points towards a dwarf galaxy, probably with irregular kinematics [65]. However, the main concern regarding Willman 1 is actually linked

DSph	$D_\odot$ (kpc)	L (10^3 $L_\odot$)	M/L ratio	Reference	Best IACTs	Observed?
Segue 1	23	0.3	>1000	[60]	M, V	M
Sagittarius	24	58000	25	[68, 69]	H	H
UMa II	32	2.8	1100	[70]	M, V	-
Willman 1	38	0.9	700	[70]	M, V	M,V
Coma Berenices	44	2.6	450	[70]	M, V	-
UMi	66	290	580	[68]	M, V	W,V
Sculptor	79	2200	7	[68]	H	H
Draco	82	260	320	[68]	M,V	W,M,V
Sextans	86	500	90	[68]	H	-
Carina	101	430	40	[68]	H	H
Fornax	138	15500	10	[68]	H	-

Table 2. A list of dSph satellites of the Milky Way that may represent the best candidates for DM searches according to their distance and/or inferred M/L ratio (the latter rather uncertain particularly for Segue 1, UMa II and Willman 1). Dwarfs appear listed according to their distance (nearest first). Note that we included Sagittarius in the list even when it is not actually a dSph, given its traditional interest for DM searches (mainly due to its proximity). Columns (6) and (7) list, respectively, the best positioned IACT for observation and the IACT that already observed the object (in chronological order when more than one). Here, H = HESS; M = MAGIC; V = VERITAS; W = Whipple.

to the more fundamental question of whether this object is gravitationally bound or not. If Willman 1 is being disrupted by the Milky Way, the velocities are not a measurement of the object's mass. This is in contrast with Segue 1, where no evidence of disruption is observed. Thus the velocities are tracing its gravitational potential, and therefore mass modeling (though uncertain) is valid.

We show in table 2 a tentative list of those dSph galaxies that could be the best candidates for DM searches at present according to their distance and/or inferred M/L ratio. Some of them have already been observed by IACTs with no success up to now [18–25]. The same negative results were recently obtained from Fermi data at lower energies [66, 67]. Nevertheless, the search of the best target should not only be based on the expected level of the DM annihilation flux. Indeed, there are other aspects that might be crucial, such as instrumental effects (e.g., the telescope PSF), expected backgrounds in the direction of the object, uncertainties in the determination of the DM density profile, angular extension of the expected gamma signal, etc. We perform a detailed study in the next subsection, where only four out of all the dwarfs listed in table 2 were selected, mainly according to their distances and mass-to-light ratios. We chose two "classical" dwarfs, namely Draco and Ursa Minor, and two dwarfs recently discovered with SDSS data, i.e., Willman 1 and Segue 1. We took into account previous estimates of the DM annihilation flux in order to improve the selection [51, 61, 63, 71–73, 78]. The same study might be performed for the rest of dwarfs as well, but we note that the main conclusions will not probably change importantly (e.g. [71]).

3.2 Looking for the best candidate

The first step is to compute the gamma-ray DM annihilation flux profiles, as given by the astrophysical factor defined in section 2. To do so, we first need to model the DM distribution. Table 3 summarizes the parameters that describe the DM density profiles of the four dwarfs under study. In the following we give more details on the adopted halo models.

DSph	Profile	r_s (kpc)	r_t (kpc)	ρ_0 ($M_\odot$ kpc^{-3})	Ref.
Draco-cusp	Kazantzidis	1.189	1.6	3.1×10^7	[51]
Draco-core	Kazantzidis	0.238	1.6	3.6×10^8	[51]
UMi-A	NFW	0.63	1.5	10^8	[15]
UMi-B	NFW	3.1	1.5	10^7	[15]
Willman 1	NFW	0.173	0.9	4×10^8	[73]
Segue 1	Einasto	0.07	0.8	10^8	[61]

Table 3. Parameters that describe the DM density profiles of the four dwarf galaxies selected. [Note: In the draco-core case, ρ_0 is in units of $M_\odot$ kpc^{-2}.]

Halo models; tidal and core radii. In the case of Draco, we chose the two DM models presented in Ref. [51], characterized respectively by a cusp and a core in the very center of the dwarf. Both of them are of the form of a Kazantzidis DM density profile [75], which is essentially an NFW plus an exponential cut-off at large radii to account for the loss of mass due to tidal disruptions in the outskirts of the dwarf. For UMi, we followed Ref. [15] and performed our calculations for the two NFW profiles given in that study. In the case of Willman 1, we extracted the main parameters from Ref. [73]. The tidal radius r_t, however, was directly derived from the Roche criterion [76]:

$$r_t = \left(\frac{M_{dSph}}{3\ M_{MW}(< R_{dSph})}\right)^{1/3} \times D_{dSph-GC} \tag{3.1}$$

where M_{dSph} is here the mass of Willman 1 (fixed to $10^7\ M_\odot$), and $M_{MW}(< R_{dwarf})$ is the enclosed mass of the Milky Way out to the distance of the dwarf. For the latter, we assumed an NFW DM density profile for our galaxy with a virial mass of $M_{vir} = 1.07 \times 10^{12}\ M_\odot$ and a concentration of $c_{MW} = 11$ following Ref. [48]. Finally, $D_{dwarf-GC}$ is the distance from the dwarf to the Galactic Center. A similar procedure was followed for Segue 1 as well, for which we took an Einasto DM density profile with index $\alpha = 0.1$ (see eq.(2.7)). We note here that we checked the robustness of our results by varying the tidal radius of both objects. We obtained that, though important for the computation of the flux coming from the outskirts, we got exactly the same flux level in the central regions, from which the maximum contributions to the flux are expected. Therefore, the uncertainties in the flux introduced by uncertainties in the computation of the tidal radius are in practice very small and completely negligible when assuming realistic values for it.

The integral of the square of the DM density along the line of sight at all angles ranging from zero up to the angle subtended by the tidal radius diverges at angles $\Psi_0 \to 0$ both for the NFW and the Kazantzidis profiles. The usual approach is to assume a small constant DM core in the very center of the DM halo that prevents the divergence of the profile. The radius r_{core} at which the self annihilation rate $t_l \sim (\langle\sigma_{ann}v\rangle n_\chi\ r_{core})^{-1}$ equals the dynamical time of the halo $t_{dyn} \sim (G\ \overline{\rho})^{-1/2}$, where $\overline{\rho}$ is the mean halo density and n_χ is the neutralino number density, is usually taken as the radius of this constant density core [77]. We used $r_{core} = 10^{-8}$ kpc in all our computations. We found that, in the range 10^{-8} kpc $< r_{core} < 0.1$ kpc, the total flux is almost insensitive to any value below $\sim10^{-3}$ kpc. Even when r_{core} takes a value as high (and improbable for these objects) as 0.1 kpc, the total flux only changes by $\sim$10%. These results are in concordance with those found in Ref. [77] as well. The conclusion is that uncertainties coming from ignorance of the real size of the core radius will be likely negligible when assuming realistic values for it.

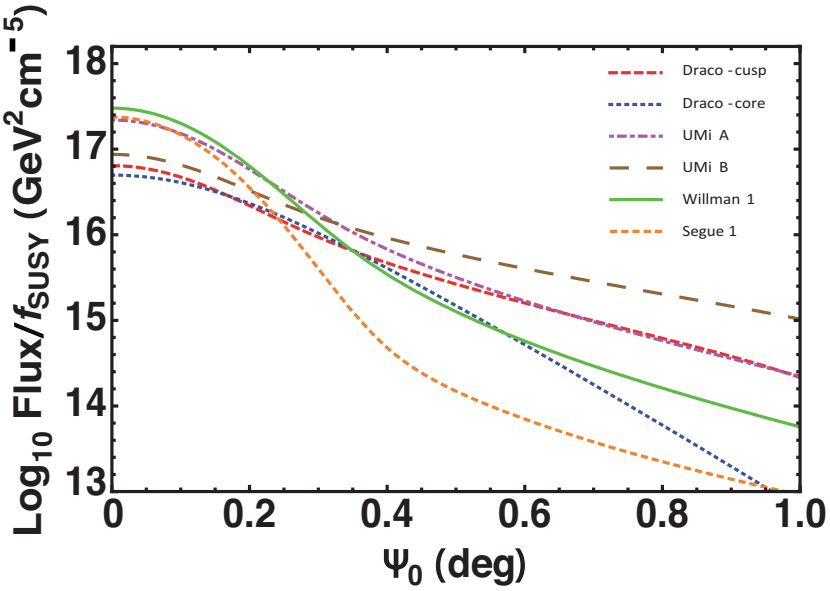

Figure 2. Gamma-ray DM annihilation flux profiles, normalized to f_{SUSY}, for Draco, Ursa Minor, Willman 1, and Segue 1. The profiles were computed using those parameters listed in table 3 for the DM distribution and assuming a PSF= 0.1°. From top to bottom at $\Psi_0 = 0°$, the profiles correspond to Willman 1, Segue 1, UMi-A, UMi-B, Draco-cusp, and Draco-core following the nomenclature given in table 3.

DSph	Log_{10} J_T ($\mathrm{GeV^2cm^{-5}}$)	ψ_{90} (deg)	r_{90}/r_s	J_{01}/J_T	r_{01}/r_s	ψ_{r_s} (deg)	J_{r_s}/J_T	Rank_{01}	Rank_{90}
Draco-cusp	17.57	0.65	0.77	0.149	0.12	0.85	0.96	5	5
Draco-core	17.48	0.43	2.53	0.148	0.59	0.17	0.36	6	6
UMi-A	17.92	0.47	0.86	0.221	0.18	0.55	0.93	3	2
UMi-B	17.85	0.87	0.32	0.108	0.04	2.69	1.00	4	3
Willman 1	17.93	0.31	1.18	0.292	0.38	0.26	0.84	1	1
Segue 1	17.71	0.23	1.34	0.369	0.58	0.17	0.74	2	4

Table 4. Value of the parameters that describe the characteristics of the DM-induced gamma emission in our sample of dwarf galaxies. See section 2.1.1 for details on their definition and usefulness. This table was computed assuming a PSF= 0.1°.

Flux profiles and role of the PSF. The flux profiles of the four dwarfs are shown in figure 2. They were computed assuming PSF = 0.1° and a DM distribution described by those parameters listed in table 3 for each particular dwarf. From this figure, we can see that, according to the gamma-ray annihilation flux profiles, Willman 1 is the best candidate, since it reaches the highest annihilation fluxes at the center. Indeed, it reaches a factor of ∼1.3 more flux than the second best candidate, Segue 1, and a factor 1.4 more than UMi-A. These three cases share therefore very similar fluxes, while the others show a central flux which is more than a factor 3 lower in the best case (UMi-B). We recall, however, that these results should be treated with caution, as the DM modeling of Willman 1 and Segue 1 may be subject to large uncertainties.

We further compute the parameters defined in section 2.1.1 and give them in table 4. According to both Rank_{01} and Rank_{90} in this table, Willman 1 represents the best choice.

PSF (deg)	J_{r_s}/J_T	ψ_{90} (deg)	Flux($< 0.1^\circ$)/ Total flux
0.01	0.97	0.63	0.29
0.1	0.96	0.66	0.15
0.3	0.89	0.86	0.04
1	0.29	1.01	0.01

Table 5. Effect of the PSF on the *apparent* distribution of the annihilation flux as may be observed in the Draco dwarf, using the cuspy DM density profile of table 3. The larger the value of the PSF, the larger the size of the region where 90% of the flux is *apparently* emitted and the smaller the observed flux in the inner 0.1°. See text for details.

Note that Segue 1 arises as the second best candidate according to its J_{01}, while it represents only the fourth best choice according to Rank_{90}. This is mainly due to the interplay between the DM distribution inside the objects, their distances, and especially the PSF of the IACT, which modifies the compactness of the signal emission and in this case leads to this interesting result.

Actually, the PSF plays a crucial role in correctly interpreting a possible DM annihilation signal. For instance, in Ref. [51] the authors showed that it might be impossible to differentiate between a cuspy and a cored DM density profile in the case of having an insufficiently good PSF for Draco. Therefore, since the PSF drastically modifies the observed flux profiles, understanding how the flux is *apparently* distributed in the object for a given PSF value becomes a crucial task. For example, we mentioned above that, assuming an NFW profile, typically 90% of the flux comes from the region inside r_s (see table 4). However, this is only strictly valid for ideal instruments where the PSF is ideally small. In practice, the larger the value of the PSF the larger the size of this region. Similarly, the observed annihilation flux coming from the inner 0.1° will decrease when worsening the PSF. To illustrate this point, we show in table 5 the result of assuming different PSFs on the values of J_{r_s}, ψ_{90} and the flux from the inner 0.1°. We chose the Draco-cusp case for this example.

Another important fact that can be read from table 4 is that dwarf galaxies are not point-like according to the morphology of their annihilation signal. In particular, we find that J_{01}/J_T only exceeds 30% in the case of Segue 1, meaning rather extended emissions in all cases. Therefore, the typical assumption of treating dwarf galaxies as point-like sources seems not to be very well founded and this fact should be ideally taken into account when analysing IACT data.

A final question to be addressed here refers to how important are the uncertainties introduced in the computation of the DM annihilation flux due to an incomplete knowledge of the real DM density profile. Implicitly, this was already done by assuming different DM density profiles for the same object (Draco and UMi). From table 4 and figure 2, we conclude that the maximum of the annihilation flux (i.e., its value at $\Psi_0 = 0^\circ$) does not vary by more than a factor 1.3 between the cuspy and cored DM density profiles considered for Draco, and a factor 2.5 for the UMi-A and UMi-B models, respectively. As for J_{01}, probably the most relevant parameter, the ratios are basically the same, i.e., 1.2 and 2.4 respectively. There are also other ways to quantify this issue. In figure 3 we performed the exercise of placing Draco (using the cuspy profile), UMi (model UMi-A), Willman 1 and Segue 1 at the same distance. We chose two distances: 23 kpc (Segue 1 real distance) and repeated the exercise for 80 kpc as well (Draco distance). Note that, though with different masses and different DM density profiles, all these dwarfs intriguingly show roughly comparable fluxes. More precisely, the

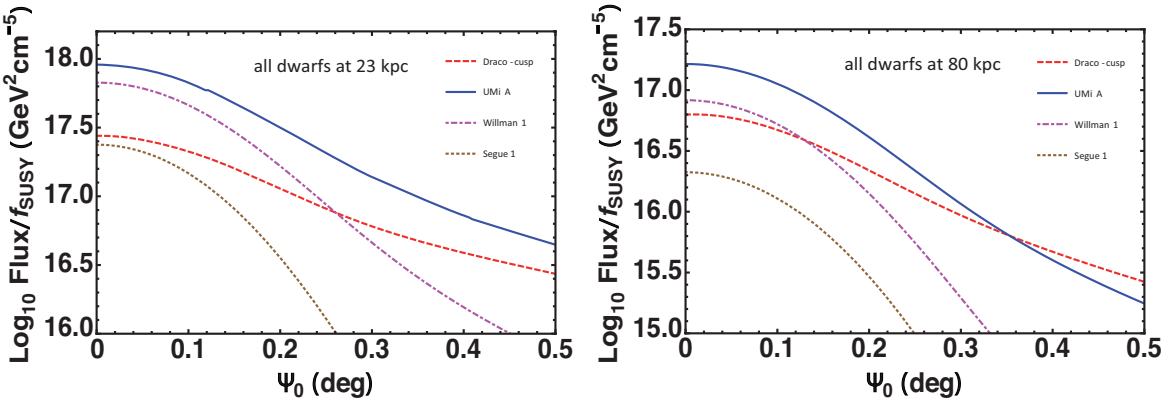

Figure 3. *Left panel:* DM annihilation flux profiles (normalized to f_{SUSY}) for Draco-cusp, UMi-A, Willman 1 and Segue 1 in the case of placing all of them at a distance of 23 kpc (Segue 1 distance). *Right panel:* All dwarfs placed at 80 kpc (Draco distance). Differences in flux, although relevant, do not exceed a factor of a few both for the maximum annihilation flux reached at $\Psi_0 = 0°$ and for the value of J_{01}; see text for discussion.

maximum differences in flux (i.e., between UMi-A and Segue 1) at $\Psi_0 = 0°$ are a factor ∼4 and ∼8 in the case that they are located at 23 and 80 kpc respectively. The situation is rather similar when dealing with J_{01}, for which we obtain maximum differences of ∼6 and ∼9 in the case of placing UMi-A and Segue 1 at 23 and 80 kpc, respectively. The reason for these relatively small uncertainties introduced by the lack of knowledge of the exact DM density profile is probably that all these objects are dSph galaxies and therefore all share roughly similar physical properties. This is true at least for those parameters which are more relevant for the computation of the DM annihilation flux, namely ρ_0 and r_s, which depend directly on the amount and distribution of matter in the innermost regions of these galaxies [58].

4 DM searches in galaxy clusters

4.1 The selection of our sample

In the currently accepted ΛCDM cosmological model, large-scale structures grow hierarchically through the merging of smaller systems into larger ones (e.g. [79]). With masses of the order of 10^{14}-10^{15} $M_\odot$ and radii of few Mpc, clusters of galaxies are the latest and most massive gravitationally bound objects to form in the Universe. Their mass is constituted principally of galaxies, gas and DM for roughly 5, 15, and 80%, respectively (see Ref. [80] for a review). No clusters have yet been detected as gamma-ray sources, however they are expected to be significant gamma-ray emitters through conventional physical processes (see, for example, the review of Ref. [81] and also [82] for recent predictions). For DM purposes, it will be necessary to understand and to model this non-exotic emission in order to discriminate it from a possible DM annihilation signal.

Some observations of clusters have been performed by the IACTs currently in operation, but only upper limits (ULs) have been obtained: from MAGIC on Perseus [83]; from HESS on Coma [84, 85], Abell 496, and Abell 85 [86]; from Whipple on Perseus and Abell 2029 [87]; from VERITAS on Coma and Perseus [88, 89] and from CANGAROO on Abell 3667 and Abell 4038 [90]. All of them were preceded by EGRET ULs at lower energies [91]. The

Cluster	z	D_L	M_{200}	R_{200}	c_{200}	r_s	ρ_0	Best IACTs	Observed?
(1)	(2)	(3)	(4)	(5)	(6)	(7)	(8)	(9)	(10)
Perseus	0.0183	77.7	7.71	1.90	3.99	0.477	7.25	M,V	W,V,M
Coma	0.0232	101.2	13.84	2.30	3.78	0.609	6.44	M,V	H,V
Ophiuchus	0.0280	122.6	23.16	2.74	3.60	0.760	5.81	H	-
Virgo	0.0036	15.4	5.6	1.68	4.21	0.433	6.81	M,V,H	-
Fornax	0.0046	19.8	1.01	0.96	4.80	0.201	11.0	H	-
NGC5813	0.0064	27.5	0.27	0.62	5.42	0.115	14.5	M,V,H	-
NGC5846	0.0061	26.3	0.38	0.69	5.26	0.132	13.5	M,V,H	-

Table 6. Main physical parameters of the galaxy clusters selected for this study. *Columns*: (1) Cluster name; (2) redshift; (3) Luminous distance in Mpc; (4) M_{200} in units of $10^{14} M_{\odot}$; (5) R_{200} in Mpc; (6) c_{200} calculated assuming the $c_{200}(M_{200})$ relation given in Ref.[97] for relaxed DM halos; (7) scale radius in Mpc; (8) ρ_0 in units of 10^{14} $M_{\odot}$ Mpc^{-3}. An NFW DM density profile was assumed to derive r_s and ρ_0; (9) Best positioned IACT for observation: H = HESS; M = MAGIC; V = VERITAS; W = Whipple; (10) IACT that already observed the object (in chronological order when more than one). *References*: (2) and (4)-(5) from Ref. [95] for all the clusters but Virgo, for which we used the M_{102} and R_{102} values given in Ref. [96], that were later converted to the M_{200} and R_{200} given above.

Fermi collaboration has already set ULs to the photon flux in the range 0.2–100 GeV for a sample of 33 promising galaxy clusters using 18 months of Fermi/LAT data [92], and it has analyzed some of them in the context of DM searches [93].

Table 6 shows our sample of galaxy clusters and their physical parameters. These clusters were selected mainly according to their distance and mass but also taking into account a good knowledge of those parameters needed to compute the DM density profiles, which were modeled here using the NFW profile in all cases. Moreover, we followed [94] in order to select the galaxy clusters that may be most interesting for gamma-ray DM searches. In that study, the authors calculated the DM-to-cosmic ray gamma-ray emission (see section 4.4) for the 110 clusters contained in the extended HIGFLUCS catalog [95]. Their conclusion is that NGC5846 and NGC5813 reach the highest ratios, therefore probably representing the best galaxy clusters to look for DM. Both clusters are included in our sample for this reason. In addition, they identified Fornax as the best target according to its expected DM annihilation flux only, and so we also included it in our study. Finally, we also picked Perseus, Coma, and Ophiuchus, even though they are not so well considered according to these rankings. However, these galaxy clusters, plus Virgo, have traditionally captured a great deal of attention both in observational campaigns and theoretical studies of diverse natures, given their proximity and masses. Therefore, they were selected for our galaxy cluster sample as well.

4.2 Looking for the best candidate

Figure 4 shows the flux profiles for the sample of galaxy clusters calculated using the parameters listed in table 6. Virgo is the galaxy cluster that yields by far the highest DM annihilation fluxes at all angles Ψ_0 in our sample. Fornax is the second best candidate, while Perseus, Ophiuchus and Coma, which show very similar DM annihilation flux profiles despite their different distances, are below Fornax by a factor of a few in the central regions. Finally, the two NGC clusters in the sample are the clusters that yield the lowest fluxes, these being already more than an order of magnitude below Virgo at $\Psi_0 = 0°$.

In table 7 we report the values of the benchmark quantities defined in section 2.1.1. There are no surprises with respect to figure 4 regarding the best and worst candidates in the

Cluster	Log_{10} J_T ($\mathrm{GeV^2cm^{-5}}$)	ψ_{90} (deg)	r_{90}/r_s	J_{01}/J_T	r_{01}/r_s	ψ_{r_s} (deg)	J_{r_s}/J_T	Rank_{01}	Rank_{90}
Perseus	16.25	0.31	1.08	0.323	0.35	0.29	0.88	3	3
Coma	16.18	0.34	0.99	0.312	0.29	0.34	0.90	5	5
Ophiuchus	16.22	0.35	0.98	0.318	0.28	0.36	0.91	4	4
Virgo	17.37	1.45	0.90	0.113	0.06	1.61	0.92	1	1
Fornax	16.58	0.55	0.94	0.214	0.17	0.58	0.91	2	2
NGC5813	15.82	0.29	1.22	0.313	0.42	0.24	0.83	7	7
NGC5846	15.97	0.32	1.12	0.297	0.35	0.29	0.87	6	6

Table 7. Value of the parameters that describe the characteristics of the DM-induced gamma emission in our sample of galaxy clusters. See section 2.1.1 for details on their definition and usefulness. This table was computed assuming a PSF= 0.1°.

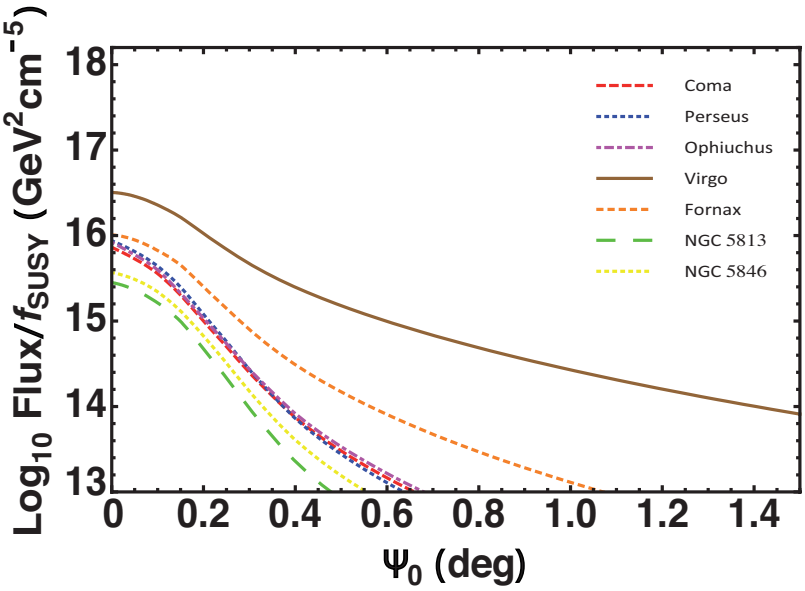

Figure 4. Gamma-ray DM annihilation flux profiles, normalized to f_{SUSY}, for Virgo, Fornax, Perseus, Ophiuchus, Coma, NGC5846 and NGC5813 (from top to bottom at $\Psi_0 = 0°$). The profiles were computed using those parameters listed in table 6 for the DM density profiles and assuming a PSF $= 0.1°$.

sample (see Rank_{01} and Rank_{90}). Probably, the main conclusion that can be extracted from this table is that we should expect the induced gamma-ray DM emission in these objects to be quite extended for IACTs, as ψ_{90} (or alternatively ψ_{r_s}, which contains in most cases ∼90% of the flux) is typically larger than 0.3°, i.e., three times the usual PSF of these instruments. Indeed, the inner 0.1° rarely encloses more than ∼30% of the total DM annihilation flux (see J_{01}/J_T). We note that rather similar results were achieved for dwarfs as well (see table 4).

4.3 The effect of substructure

In the ΛCDM paradigm, the smallest dense halos form first and later merge to originate larger structures. This hierarchical scenario has as a direct consequence the presence of a large amount of substructure in CDM halos. As the DM annihilation signal is proportional to the DM density squared, this clumpy distribution of sub-halos inside larger halos may

boost the DM annihilation flux considerably. The flux enhancement will be more important for the most massive halos as they enclose more hierarchical levels of the structure formation. Therefore, it becomes essential to quantify precisely the substructure boost when computing the DM annihilation flux from galaxy clusters. In contrast, the effect will turn out to be insignificant for dwarfs.

The effect of substructures on the DM annihilation flux has already been studied both analytically (e.g., in Refs. [61, 98, 99]), and making use of state-of-the-art N-body cosmological simulations [100, 101], although the exact calculation of the substructure boost has been challenging. It becomes quite difficult to calculate analytically the survival probabilities of substructures within the host halos, while the most powerful N-body simulations fail to simulate the sub-halo hierarchy below a mass $\sim 10^5 M_\odot$, still very far from the minimum halo mass predicted to be present in the structure formation scenario, of the order of $10^{-6} M_\odot$ or even smaller [102].

Recently, Kamionkowski, Koushiappas, and Kuhlen developed in Ref. [26] a semi-analytical model in order to include the substructure in the computation of the DM annihilation flux (hereafter 3K10 model). Their model is based on a previous analytical study that described the self-similar substructure expected from hierarchical clustering [103]. The 3K10 model makes an upgrade of this first work by performing a calibration to the Via Lactea II N-body cosmological simulation [104]. After this calibration it is possible to use the model to obtain a suitable extrapolation of the results of the simulation below its lower mass limit. In addition, the 3K10 model includes a good description of the distribution of substructure in the halo when varying the galactocentric radius. Both achievements make possible a more realistic and precise computation of the substructure boost to the DM annihilation flux. The 3K10 model indicates that the lower mass halos will not contribute greatly to this boost.

In the 3K10 framework, the boost factor $B(r)$ is given by:

$$B(r) = f_s e^{\Delta^2} + (1 - f_s)\frac{1+\alpha}{1-\alpha}\left[\left(\frac{\rho_{max}}{\rho(r)}\right)^{1-\alpha} - 1\right]. \tag{4.1}$$

where f_s refers to the volume of the halo that is filled with a smooth dark matter component with density ρ(r), while the fraction $(1-f_s)$ corresponds to a high-density clumped component due to the presence of substructures. We chose $\Delta = 0.2$, $\alpha = 0$ and $\rho_{max} = 80$ GeV cm^{-3}, which are the values found when calibrating the 3K10 model to the VL-II simulation. We refer the reader to Ref. [26] for a detailed description of each of these terms. Note that the boost factor is indeed composed of two terms: a first term $B_s = f_s e^{\Delta^2}$ due to the finite width of the smooth component (that will have little importance here) and a second term due to substructures.

We can also numerically evaluate the total boost from substructure within a radius R:

$$B(<R) = \frac{\int_0^R B(r)\,\rho^2(r)\,r^2\,dr}{\int_0^R \rho^2(r)\,r^2\,dr}. \tag{4.2}$$

By applying the 3K10 methodology, we assume to be independent of the host halo mass and the properties of the sub-halo population. The only uncertainty would come from the parameters of the model, especially from f_s, which is related to how effective tidal stripping (or any other sub-halo destroying mechanism) is. In the 3K10 formalism, f_s(r) was determined from VL-II, but the simulations are many orders of magnitude away from resolving the whole sub-halo hierarchy, and therefore f_s is not known with unlimited precision.

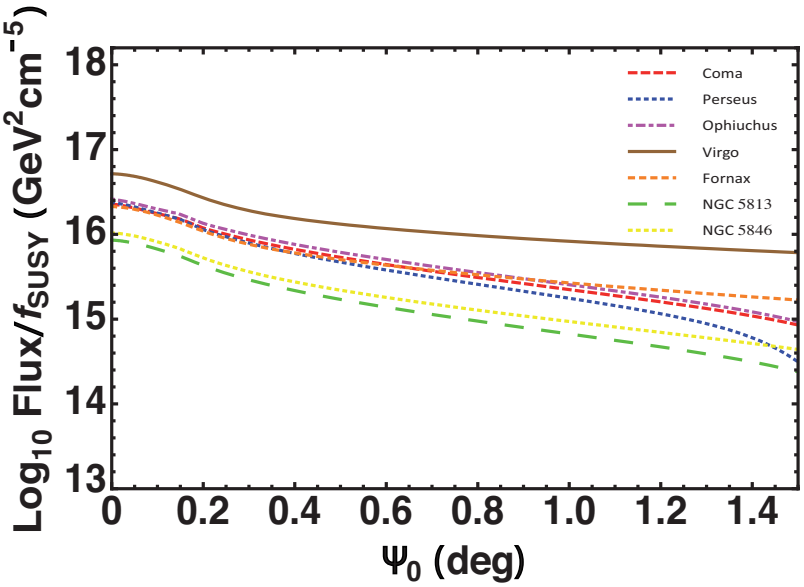

Figure 5. Gamma-ray DM annihilation flux profiles, normalized to f_{SUSY}, for Perseus, Coma, Ophiuchus, Virgo, Fornax, NGC5813, and NGC5846. The profiles were computed using those parameters listed in table 6 for the DM density profiles and assuming a PSF=0.1°. Substructure is included here following the 3K10 model [26] using those parameters given in the text. From top to down at $\Psi_0 = 1.2°$, the profiles correspond to Virgo, Fornax, Ophiuchus, Coma, Perseus, NGC5846, and NGC5813.

On the other hand, our intention is to apply the 3K10 formalism to dwarf galaxies and galaxy clusters and not only to MW-sized objects, so it is necessary to rescale f_s(r) in order to correctly accommodate it to halos of different sizes. We do so by replacing the $\rho(r = 100\,\mathrm{kpc})$ parameter in eq.(4) of Ref. [26] by $\rho(r = 3.56 \times r_s\ \mathrm{kpc})$, i.e.:

$$1 - f_s(r) = 7 \times 10^{-3} \left(\frac{\rho(r)}{\rho(r = 3.56 \times r_s\ \mathrm{kpc})} \right)^{-0.26}, \tag{4.3}$$

as 3.56 is the ratio between the VL-II scale radius ($r_s = 28.1$ kpc) and $r = 100$ kpc (value extracted *ad hoc* from VL-II to properly calibrate the 3K10 model). Note that in doing so we are assuming the same radial dependence of f_s for all halo masses, only rescaling it to the particular size of the new object.

In figure 5 we show the result of applying the 3K10 model to our sample of galaxy clusters using the values given above for f_s, ρ_{max}, and α, as well as the new scaling relation introduced in eq. (4.3). The substructure boost turns out to be extremely important in all cases, its effect being relevant at all l.o.s. angles Ψ_0. Note that the largest flux enhancements, however, are achieved at the largest Ψ_0 (compare with figure 4). Furthermore, Ophiuchus, Perseus, and Coma are now at the same flux level as Fornax. The quantitative analysis is summarized in table 8. $Rank_{01}$ and $Rank_{90}$ are now significantly altered with respect to table 7. The total boost within the virial radius gives us an idea of the global importance of substructure for each object: typical values of this boost for the most massive halos in the sample are of the order of 50.

Yet, there are important observational consequences that arise when comparing tables 7 and 8: J_{r_s}/J_T rarely reaches values greater than 0.2 when including substructure, in contrast

Cluster	B($< R_{vir}$)	Log_{10} J_T ($\mathrm{GeV^2cm^{-5}}$)	ψ_{90} (deg)	$\mathrm{r}_{90}/\mathrm{r}_s$	$\mathrm{J}_{01}/\mathrm{J}_T$	$\mathrm{r}_{01}/\mathrm{r}_s$	ψ_{r_s} (deg)	$\mathrm{J}_{r_s}/\mathrm{J}_T$	Rank_{01}	Rank_{90}
Perseus	34.0	17.73	1.22	4.24	0.037	0.14	0.29	0.19	3	5
Coma	51.6	17.84	1.41	4.08	0.028	0.29	0.34	0.20	4	4
Ophiuchus	54.0	17.89	1.38	3.89	0.028	0.28	0.36	0.21	2	3
Virgo	55.0	19.11	7.29	4.55	0.004	0.06	1.61	0.18	1	1
Fornax	39.9	18.17	2.97	5.11	0.013	0.17	0.58	0.16	5	2
NGC5813	34.8	17.33	1.36	5.69	0.035	0.42	0.24	0.14	7	7
NGC5846	36.1	17.51	1.59	5.54	0.028	0.35	0.29	0.15	6	6

Table 8. Same as table 7 but now including substructure. B($< R_{vir}$) is the total boost within the virial radius of the object, as given by eq. (4.2). This table was computed assuming a PSF$= 0.1^\circ$.

with the typical values $\sim$0.9 found without substructure. This means that the gamma-ray DM annihilation induced emission is indeed even less concentrated than previously thought, the object being significantly more extended for IACTs. We note that this fact already has important implications, e.g., on those conclusions achieved in Ref. [83] regarding DM searches in Perseus with the MAGIC telescope, where the authors assumed that the majority of the flux approximately comes from a region comparable with the telescope PSF and $\mathrm{J}_{r_s}/\mathrm{J}_T = 0.9$. Other related quantities in table 8 where this same issue is clearly visible are $\mathrm{J}_{01}/\mathrm{J}_T$, which surprisingly falls below 4% for all the considered objects, and $\mathrm{r}_{90}/\mathrm{r}_s$, now of the order of 4–5 in contrast to the previous factor $\sim$1. Indeed, table 8 shows that ψ_{90} is, in all cases, somewhat greater than 1°, clearly indicating the distinct extended nature of the gamma-ray emission. Similar conclusions have also been obtained in recent works adopting different substructure treatments [31, 105]. They found, however, much larger substructure boost factors (roughly a factor 20 higher) than those given in our table 8.

For completeness, we also studied the effect of substructure on our sample of dwarf galaxies, although, as mentioned, its importance is expected to be negligible for these objects. Effectively, we found the following values for the total boost, as given by eq. (4.2), within the tidal radius: 1.12, 1.12, 1.16, 1.16, 1.19, 1.31 for Segue 1, Willman 1, UMi-A, UMi-B, Draco-cusp, and Draco-core respectively. The DM annihilation flux profiles are not significantly affected by introducing substructure either, except marginally in the outer regions, where in any case the level of the flux still remain extremely low.

4.4 γ-rays with a non-DM origin in clusters

When considering DM searches in galaxy clusters one has to carefully consider the possible emission from other non-DM sources. In first place, some clusters contain bright active galactic nuclei (AGN) [106] that may hinder the possible DM detection. These sources, while often detected at Fermi-LAT energies [107], are not always observed in the GeV-TeV range. This is due to the high-energy emission cut-off given by the decreasing inverse Compton (IC) scattering efficiency in the Klein-Nishina regime. Moreover, in this sense, the AGN jet inclination angle and the gamma-ray absorption in the source neighborhood also play an important role. However, many AGN are proved to emit efficiently at very high energies and, additionally, they typically show variable emission. Therefore, no general conclusions on their impact on cluster DM searches can be drawn and their emission should be carefully modeled in order to correctly derive implications for DM (see Ref. [37]). Alternatively, AGN could be masked away as they are typically point-like objects for IACTs.

Another source of gamma-rays in clusters that can frustrate DM searches are cosmic

rays (CR). CR electrons are directly visible in many galaxy clusters via synchrotron radiation in radio, forming the so-called cluster radio halos [108]. These particles can be injected into the intra-cluster medium (ICM) by various sources such as structure formation shocks, radio galaxies and supernovae driven galactic winds (see the introduction of Ref. [83] and reference therein). The same sources can also inject CR protons into the ICM. Both CR protons and electrons can generate high-energy gamma-ray emission, via pion-decay [109–114] and IC up-scattering of the cosmic microwave background [115–119], respectively. A detailed discussion of these particles and their relative contribution to the gamma-ray emission is beyond the scope of this study and we refer the reader to the above references as well as to Ref. [82] and references therein. Additionally, see also Ref. [121] for the effect of turbulence on merging clusters that can also accelerate CRs to very high-energies.

State-of-the-art cluster cosmological simulations show that the dominant contribution to the CR induced gamma-ray emission, at the energies of interest here, should come from pion-decay [82, 113]. Spatially, this emission is concentrated in the inner part of the cluster as it is proportional to the squared ICM density. On the other hand, in this study we showed that 90% of the DM emission in a cluster typically comes from within a radius of $\sim 0.3^\circ$ (or larger) that dramatically changes to $\sim 1.2^\circ$ (or larger) when including the substructure treatment (see tables 7 and 8).

One might think that the expected DM-induced emission spatial profile would be comparable to the CR-induced one, but, in a realistic scenario that correctly includes substructures, the former is clearly more extended and has a shallower profile (see for comparison fig. 13 of Ref. [82] and the recent [31]). In practice, given that a typical Cherenkov telescope PSF is $\sim 0.1^\circ$, it is hard to imagine that existing IACTs will be able to distinguish between CR and DM from the emission spatial profiles (this may change with the next-generation Cherenkov Telescope Array). Fortunately, the spectral profile of the CR-induced emission also helps. In the energy regime of interest for IACTs, between 50 GeV and few TeV, this emission is expected to follow a power-law spectrum with a spectral index of -2.2 [82] while the latter is expected to be harder (-1.5 or more) when having a DM origin. Therefore, should the DM annihilation emission be comparable to the CR induced one, the very peculiar characteristics of the former would be hopefully recognizable against the latter.

5 DM annihilation flux predictions and detection prospects for IACTs

5.1 Galaxy clusters or dwarf galaxies?

In this section, we will compare the results previously obtained for dwarf galaxies with those obtained for galaxy clusters with the aim of elucidating the best candidates for gamma-ray DM searches. The result of the comparison is given in figure 6, where we show the case with no substructure at all (left panel) and a second case where we included substructure, in both dwarfs and clusters (right panel). For clarity, we do not use our whole sample of objects, but just the sub-sample composed by those three dwarfs —Willman 1, Segue 1 and UMi-A— and three clusters —Virgo, Fornax and Ophiuchus— with the highest fluxes.

In both panels, dwarf galaxies reach the highest flux levels at $\Psi_0 = 0^\circ$, roughly an order of magnitude larger than those expected from clusters. This therefore seems to favor dwarfs against galaxy clusters, particularly for point-like based observational search strategies. However, note that galaxy clusters dominate the gamma-ray DM-induced emission at large angles once substructure is properly taken into account. This happens at radii greater than $\sim 0.4^\circ$

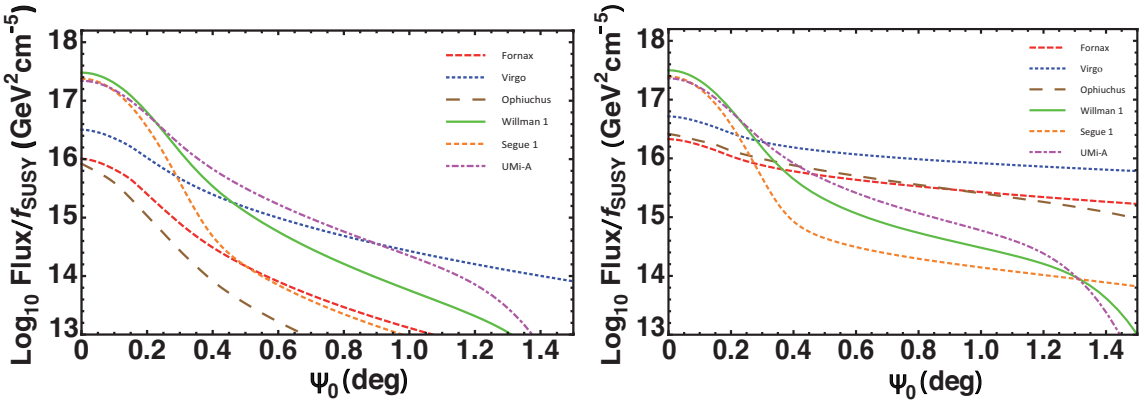

Figure 6. *Left panel:* Comparison of the DM annihilation flux profiles (normalized to f_{SUSY}) for the subsample of those three dwarfs and three clusters with the highest fluxes. *Right panel:* Same as left panel but this time including substructure following the 3K10 model described in section 4.3.

in all cases, fluxes remaining substantially higher than those expected from dwarfs and decreasing quite slowly up to very large radii, contrary to what happens in dwarfs. Actually, once we include the effect of substructure, some of these galaxy clusters emit much more DM annihilation flux *in total* than the best dwarf galaxies. For example Virgo, as can be seen by comparing J_T in tables 4 and 8, gives a flux larger than Willman 1 by a factor $\sim$13. However, the main contribution to the total flux now comes from the outer regions, where the flux level is comparatively quite low with respect to that reached in the very center. Thus, if our search strategy can deal with quite extended sources (meaning $\sim 1-1.5^\circ$, which, as shown in table 8, is the typical value of ψ_{90}, i.e., the typical size of the 90% emitting region), then galaxy clusters probably are the best candidates or at least represent good competitors to dwarfs.

5.2 J-values comparison with other works

Below we comment on the agreement/disagreement of our J-values with those found in some works in the literature. We note that, when performing such a comparison, one has to be very careful in dealing with the different notations and definitions (see e.g. Appendix A in ref. [124] for a useful discussion on conversion units and related issues).

- Dwarfs:
  - In the classical work of Ref.[14], authors found a J_{01} for Draco which is roughly a factor 1.5 higher than the one given in our table 4 for the Draco-cusp case.
  - After correcting by different definitions and angular apertures, we found ref. [122] to predict a slightly lower J_{02} value (i.e. eq. (2.9) with $\psi = 0.2^\circ$) for Willman 1; more precisely they found 8% less flux than the one we find. As for UMi-A, we obtain a slightly higher J_{01} value.
  - We obtain similar J_{01} values for UMi-A and UMi-B than those given in Ref. [71]. However, we end up with significantly lower values for Draco. The found difference is completely attributable to the different halo parameters used in each case.
  - Authors in ref. [78] find a J_{01} value for Segue 1 which is a factor 1.6 larger than the one given in our table 3.

- Our J_T values for both Draco and Willman 1 are in good agreement with those given in ref. [72] for the same objects. More precisely, authors in that work find Draco and Willman 1 to yield a factor 1.1 and 1.3 more DM annihilation flux respectively.
- The MAGIC collaboration used a J_{01} value for Segue 1 in ref. [24] that is a factor 2.8 higher than the one given in this work. These differences are due to the slightly different halo parameters used in each case.
- The results shown in our table 3 for both Draco-cusp and UMi-A match perfectly with those given in the recent ref. [124] for the same objects.

- Clusters: In case of clusters, only absolute flux values have been quoted in the scarce literature available so far, rather than providing J-values for them. Thus, a one-to-one comparison is not straightforward as one may take into account the particular particle physics model used in each case. Below, we perform just a qualitative comparison.
  - Ref. [94] ranks the galaxy clusters according to their expected DM annihilation flux in their table VIII. Limiting here the comparison to those clusters that are common to both works, they found, starting from the brightest, the following: Fornax, Ophiuchus, Coma, Virgo, Perseus, NGC5846, NGC5813. In our work, we find (with substructure, table 8): Virgo, Fornax, Ophiuchus, Coma, Perseus, NGC5846, NGC5813. Therefore, except for Virgo, for which we find a higher flux, both works share a similar ranking list. On the other hand, note that, although authors in ref. [94] quoted NGC5846 and NGC5813 as the best ones for DM searches given their comparatively low cosmic ray induced gamma-ray emission (see their Fig.16), our results are actually perfectly compatible. Attending *only* to their DM annihilation flux, both galaxy clusters are not by far the most promising ones for DM searches, neither in [94] nor in our work.[7]
  - Ref. [31] summarizes in their table 1 absolute fluxes for different galaxy clusters. For their model BM-K', they find that, above 100 GeV, Virgo yields the highest flux level, followed by Fornax, Perseus and Coma. This is perfectly compatible with our results. However, total fluxes are roughly a factor 40 higher in all cases. The differences are mainly due to different substructure treatments, which lead to rather different substructure boosts, as well as to the inclusion of the Sommerfeld effect, which was not considered here.
  - To our knowledge, ref. [105] is, together with the present work, the only one in the literature that compares in some detail dwarfs and clusters in the context of DM annihilation. However, it is hard to compare it with our results, as they refer their fluxes to what it is found in N-body cosmological simulations. Qualitatively speaking, both works agree on the fact that Willman 1 is brighter than Draco, and Fornax more promising than Coma. On the other hand, we remind that we find substantially lower substructure boost factors (a factor $\sim$20), and therefore we do not find clusters to be best targets than dwarfs *always*, as they do. In our

[7] In any case, we found it convenient to include both NGCs in our cluster sample and discuss their flux predictions in the context of a joint study dwarfs+clusters, keeping in mind that, as we do not perform a treatment of the cosmic ray induced gamma-ray emission in clusters, both NGCs will be clearly disfavored when only studying DM annihilation.

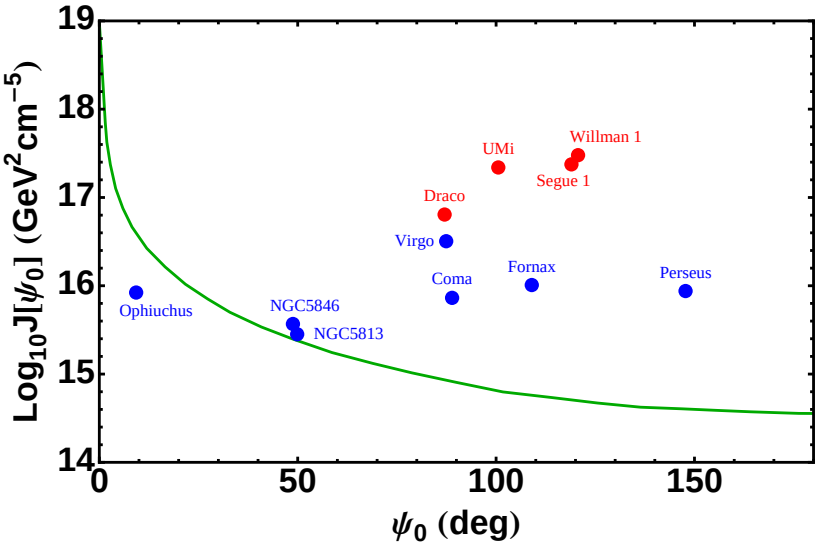

Figure 7. DM annihilation flux profile of the MW halo versus the J_{01} values of dwarfs (red points) and clusters (blue points). No substructure boosts are included in the plot. The MW flux profile (green line) was computed assuming a PSF = 0.1°. Note that all the objects are above the MW flux profile but Ophiuchus, which surprisingly is well below. The latter will not change by including substructures, as they have a negligible impact in the inner 0.1°.

case, the exact ranking is indeed rather sensible to the set of parameters that we select in order to plan the observational search strategy (see section 5.1).

5.3 Milky Way foreground

Yet, we did not take into account the apparent position of the objects with respect to the Galactic Center. This issue might turn out to be relevant, as we should expect an important contribution to the gamma-ray flux coming from DM annihilations in the MW halo, which in this sense might act as a foreground. Nevertheless, the DM annihilation coming from the MW halo should not be considered in this way. Indeed, strictly speaking, it should be treated as an additional signal that would sum up to the expected signal from each of the objects in the sample. Note also that both signals would have the same energy spectrum.

Figure 7 shows the DM annihilation flux profile of the MW halo compared to the J_{01} values of both dwarfs (red points) and clusters (blue points) as extracted from tables 3 and 7 respectively. We did not include substructure with the intention to be conservative. The MW flux profile, given by the green line, was computed assuming a PSF = 0.1°. Note that all the dwarfs in our sample are well above the MW flux profile. In the case of galaxy clusters, however, only Coma, Fornax, Perseus and Virgo are indeed well above. NGC 5813 and NGC 5846 are just slightly above. And, surprisingly, Ophiuchus is *well below* the level of the MW halo, the main reason being the fact that it is only $\sim 9°$ away from the Galactic Center in the sky. This result will not change even if we had included the effect of substructures, as we remind it has little relevance for the inner 0.1°. Therefore, Ophiuchus is not probably a good candidate after all, as its DM annihilation flux is expected to be completely embedded in the MW foreground (with the PSF used here; see below for further discussion).

On the other hand, from an observational point a view, it might be this MW foreground that better defines the outer extent of the objects in our sample rather than the tidal radii

given in table 3 for dwarfs or the virial radius given in table 6 for galaxy clusters. It turns out, however, that in case of dwarfs the difference is not very important. Indeed, the level of the DM annihilation from the MW equals the one predicted for dwarfs typically at a radius that *already* encloses most of the flux (typically ∼95%). For clusters, however, this issue matters, as clusters have J_{01} values that are substantially lower than those of dwarfs (substructure will not help too much here, as they are not expected to be relevant in the inner 0.1°). Nevertheless, we note that this effect strongly depends on the integration angle used, as it can been clearly seen in figure 14 of ref. [124] for a sample of dwarfs: the smaller the integration angle the better the contrast between the object signal and the MW foreground. In any case, this fact should be taken into account when programming observational campaigns and analyzing the data. As an example, assuming integration angles of 0.1°, the MW foreground signal equals the one expected from Perseus without substructure (with substructure) at ∼0.2° (∼0.55°) away from its center. At this radius, the integrated signal is roughly 80% (40%) of the total flux.

5.4 Flux predictions

Figure 8 summarizes the detection prospects of the best objects in our joint dwarfs + clusters sample for the MAGIC telescopes and for the future Cherenkov Telescope Array (CTA; see Ref. [120]). More specifically, this Figure shows the integrated spectrum of the Willman 1 dwarf galaxy, and Perseus and Virgo galaxy clusters. We used the particle physics model labelled *B* in table 1, as this model gives the most optimistic results for a large portion of the IACT energy range (see figure 1), e.g., $f_{SUSY} = 7.2{\times}10^{-33}$ GeV^2 cm^{-5} at 100 GeV. For the astrophysical factor, we picked the J_{01} and J_{90} values given in table 4 for Willman 1, and tables 7 and 8 for Perseus and Virgo without and with substructures respectively. Virgo, which represents the best cluster according to its flux level, is extremely extended; indeed, $\psi_{90} > 7°$ in this object (see table 8), probably meaning a serious handicap for IACT observations and data analysis of a possible DM signal. In contrast, $\psi_{90} \sim 1.2°$ in Perseus, which is also rather similar to other clusters like Ophiuchus or Coma and is therefore a good representative of all of them (although Ophiuchus seems a slighter better candidate according to tables 7 and 8, we remind that this cluster is probably completely embedded in the MW foreground, which a priori makes it less appealing; see section 5.3).

Willman 1 is the best candidate when neglecting substructures, both for J_{90} and J_{01}. However, once substructures are properly included, Virgo yields the highest total flux (well described by J_{90}), although Willman 1 still remains as the best target regarding J_{01} (meaning more point-like for IACTs, as already discussed). Interestingly, Perseus is roughly at the same flux level as Willman 1 attending to their J_{90}, although it is clearly less promising than both Virgo and Willman 1 according to its J_{01}.

Figure 8 also shows the integral sensitivity curves of both the MAGIC telescopes and CTA in order to illustrate the DM search potential of both instruments. The MAGIC sensitivity line represents the flux needed to reach a 5σ significance and ≥ 10 excess event in 50 h of data [123]. As for CTA, the sensitivity curve corresponds to 50 h observation time at a zenith angle of 20°, as given for configuration *E* in Ref. [120]. We also included in figure 8 the ULs to the central flux as derived from MAGIC observations of Willman 1 in Ref. [21] using their particle physics model K' (which are also rather similar to those deduced from MAGIC observations of Segue 1 in Ref. [24] assuming a spectral index of −1.5). We also plotted the ULs derived for Perseus from MAGIC data in Ref. [83].[8]

[8] One may wonder why the MAGIC upper limits are better than the MAGIC stereo curve sensitivity. This

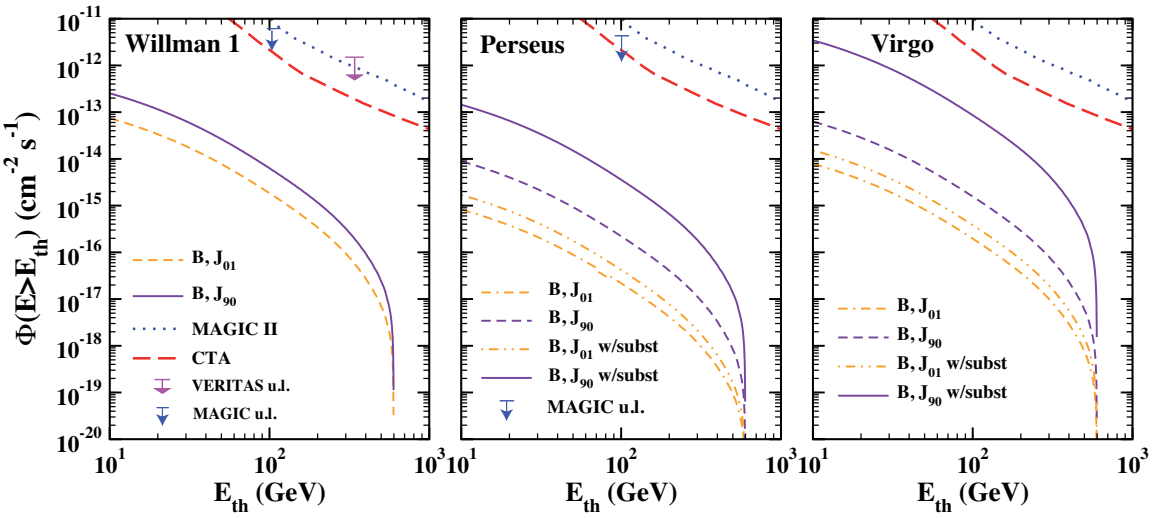

Figure 8. Integrated spectrum of the best dwarf and galaxy cluster in our sample: Willman 1 (left panel) and Virgo (right panel), respectively. Given the extremely large spatial extension of the flux in Virgo, we also included Perseus (middle panel) as a good alternative (see text for discussion). Two values of the flux are plotted, namely those corresponding to J_{01} and J_{90} astrophysical factors as given in tables 4 and 7. For Virgo and Perseus we also show the effect of substructures (table 8). We used the particle physics benchmark model labelled B in table 1 and figure 1, which gives the highest particle physics factor. The integral sensitivity curves of both the MAGIC telescopes and CTA for 50 h observation time are also shown in the panels, as well as the ULs to the flux derived from MAGIC and VERITAS observations of Willman 1 [21, 22] and Perseus [83].

A quick comparison between the expected level of the DM annihilation flux and both the sensitivity lines of the MAGIC stereoscopic system and CTA shows that it is unlikely that these instruments can detect γ-rays from DM annihilation in any of these objects (which we recall are the most promising among dwarfs and clusters), unless other effects are included that may boost the DM signal considerably. Indeed, the minimum difference between the CTA sensitivity line and the DM-induced γ-ray flux from Virgo, which occurs at $\sim$135 GeV, is still larger than an order of magnitude. For Willman 1, the situation is even worse, minimum differences being of the order of $\sim 10^3$ (note that same factors were recently achieved by the MAGIC collaboration for Segue 1 in Ref. [24]).

At 135 GeV, the value of the particle physics factor, f_{SUSY}, is $\sim 0.37 \times 10^{-32}$ GeV^2 cm^{-5}, and this is indeed the value used in figure 9 to plot the DM annihilation flux profiles (with substructure) of Willman 1, Perseus and Virgo together with both the MAGIC and CTA sensitivities at 135 GeV. This is therefore one of the most optimistic scenarios that it is possible to achieve. We also included in figure 9 Ursa Minor (model A), which is the second best dwarf according to our findings in section 3. Note that the sensitivity lines are now given for a rather optimistic deeper observation of 250 h integration time. However, for the examined particle physics model, the sensitivity lines of current and planned instruments are

can be explained by the fact that those ULs are derived for a spectral index of about -1.5, while the sensitivity curves are obtained assuming a Crab Nebula-like spectrum. Also, ULs are always expected to be better than sensitivity curves at parity of conditions.

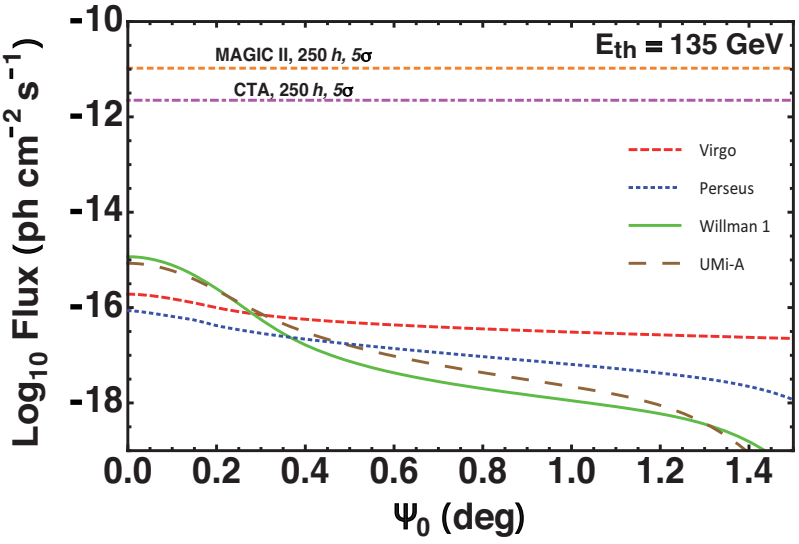

Figure 9. DM annihilation flux profiles, including substructures, of the two pairs of most promising objects in our sample, namely Willman 1 (green solid line) and Ursa Minor model A (brown dashed) among dwarf galaxies, and Virgo (red short dashed) and Perseus (blue dotted) among galaxy clusters. The sensitivities reached by MAGIC in stereo mode and CTA after a deep observation of 250 h integration time are given for comparison. Both the instrumental sensitivities and the particle physics factor, f_{SUSY}, were computed for an energy of 135 GeV, i.e., the one which gives the minimum difference between the expected flux and the sensitivity curves of the MAGIC telescopes and CTA in figure 8.

more than one order of magnitude above the predicted flux profiles.

6 Summary and conclusions

In this article, we have studied in detail the DM annihilation gamma-ray fluxes for a sample of nearby dwarf galaxies (Draco, Ursa Minor, Willman 1, and Segue 1) and nearby galaxy clusters (Perseus, Coma, Ophiuchus, Virgo, Fornax, NGC 5813, and NGC 5846), with the intention of elucidating which object class (dwarfs or galaxy clusters) is more appropriate for gamma-ray DM searches with present-day and/or planned IACTs. We have used the latest modeling of the DM density profiles, which were calculated from the latest observational data available. On the way, we have also discussed some observational and instrumental aspects that may become crucial when planning a good observational strategy as well as to posterior interpretation of IACT data. We finally studied the detection prospects of the best objects in our sample for current and planned IACTs. The main results of this work can be summarized as follows:

- Nearby galaxy clusters may yield similar, or even higher, annihilation fluxes once the effect of substructure in the DM halo is properly taken into account.

- Substructure was included following the 3K10 model [26], slightly modified here so that we could safely apply it to CDM halos of different masses rather than MW-sized halos only. We found that substructure is only relevant (and critical in most cases) for galaxy

clusters and not for dwarf galaxies, indeed enhancing the gamma-ray signal a factor ∼35-50 in clusters but only 30% at most in dwarfs.

- Willman 1 appears to be the best candidate among the dwarf galaxies as it shows both the largest J_{90} and J_{01}, as well as the highest fluxes at the center (see figure 2). Moreover, 90% of the flux is expected to come from a quite small region, i.e., $\psi_{90} \sim 0.3$ degrees, which means a quite compact emitting region, more feasibly observable with present IACTs. Yet, it is not clear whether or not this object is gravitationally bound at all, so other candidates with less mass modeling uncertainties and quite similar fluxes, such as Ursa Minor and Segue 1, would probably represent better options.

- Virgo represents the galaxy cluster with the highest fluxes both according to J_{90} and J_{01} (essentially due to its extreme proximity). However, its large spatial extension (indeed, $\psi_{90} > 7^\circ$ with substructure) can be a serious handicap for IACT observations and data analysis. Yet, other candidates with high predicted fluxes and more moderate ψ_{90} values such as Perseus or Coma may represent good alternatives.[9]

- For an integration angle of 0.1°, the DM annihilation flux level of the MW halo is well below the one predicted for the inner 0.1° of all dwarfs in the sample. This is also true for all galaxy clusters selected but Ophiuchus, located only ∼9° from the Galactic Center. This cluster appears to be completely embedded in the MW foreground, making it challenging for DM searches. The inclusion of substructures will not affect this result. In any case, we recall that the exact contrast against the MW foreground strongly depends on the integrated angle used.

- The best targets according to J_{90} do not necessarily represent the best targets according to J_{01}. An example is Segue 1, which is only the fourth best object according to its J_{90} but turns out to be the second best option according to J_{01}. This result is due to the interplay in the astrophysical factor between the object's distance, the DM distribution and the telescope PSF.

- The best dwarf galaxies in the sample have DM annihilation fluxes at $\Psi_0 = 0^\circ$ which are roughly an order of magnitude higher than those expected for the best galaxy clusters. Even when including substructure in both kinds of objects, dwarf galaxy flux profiles are higher than those of galaxy clusters typically within the inner $\sim 0.4^\circ$.

- Once substructures are included, galaxy clusters flux profiles appear to be systematically higher than those of dwarfs typically at angles $\gtrsim 0.4^\circ$ (right panel in figure 6). Indeed, the larger the l.o.s. angle Ψ_0 the larger the relative DM annihilation flux enhancement due to presence of substructure. As a consequence, the flux profiles surprisingly remain almost flat up to larger radii (of the order of ψ_{90}). The fraction of the total DM flux within r_s for galaxy clusters, J_{r_s}, now drastically decreases from ∼0.9 to ∼0.2.

- With the above given considerations in mind, dwarf galaxies are best suited for observational strategies based on the search for point-like sources, given their highest J_{01}

[9]Fornax is the best candidate according to ref. [31], as they find this cluster to have a particularly low cosmic ray induced background; however, its angular size ∼3° is roughly double that of Perseus or Coma, which still makes it rather challenging.

values and still reasonable ψ_{90} values, while galaxy clusters are the best targets for analyses that can deal with rather extended emissions (we recall, however, that neither dwarfs nor clusters are point-like according to their J_{01}/J_T values). Ideally, the regions to be analyzed in clusters should enclose at least the solid angle subtended by ψ_{90}, of the order of $\sim 1^\circ$. Given their typical flux profiles, which remain almost flat up to large radii, a suitable data analysis strategy could consist of masking those inner regions where other conventional γ-ray emission mechanisms may contaminate the DM signal.

- In the framework of the CMSSM the most optimistic f_{SUSY} value that it is possible to achieve above 100 GeV is of the order of 10^{-32} GeV^2 cm^{-5}. The level of the DM annihilation fluxes for the best objects in the joint dwarfs + clusters sample is well below the sensitivities of both current IACTs and the future CTA. Indeed, we do find minimum differences between predictions and sensitivity lines of more than an order of magnitude in the most optimistic case, i.e., Virgo with substructures at 135 GeV (see figure 8) and 50 h observation time of CTA. For Willman 1, the mismatch is above two orders of magnitude. Increasing, for example, the total IACT exposure time five times up to 250 h does not change the detection prospects substantially, as the signal-to-noise ratio increases only as the square root of time and therefore both an integrated signal (the one associated either with J_{01} or J_{90}, for instance) and the flux profiles are still far from detection.[10]

Yet, despite all the negative observational results accumulated so far, as well as the rather discouraging detection prospects we found in our analysis, there are reasons for keeping optimistic. First, we remind that our results were achieved assuming a specific particle physics framework, namely the constrained minimal supersymmetric standard model. We chose CMSSM because it represents the benchmark beyond standard model scenario expected to be probed soon (at least part of the parameter space) at the LHC. In any case, as pointed out also in Ref. [127], we note that even if the LHC does provide evidence for SUSY or if future direct detection experiments will detect a clear signature of DM, γ-ray observations provide the only way to go beyond a detection in the local DM halo, measuring the DM halo profiles and elucidating the exact role of DM in structure formation. In other models, there exist new particles and mechanisms that might boost the DM-induced γ-ray signal, e.g., Sommerfeld enhancements [29]. Other promising scenarios are also possible which deserve further detailed study, such as DM decay [125, 126].

New generation IACTs already in operation like the MAGIC stereoscopic system and the HESS upgrade,[11] or CTA in the near future, do actually improve the chances of detection significantly and, at least, should be able to impose more stringent limits on the particle physics models. The complementarity of IACT searches with those performed by Fermi/LAT at lower energies also represents a key point in order to achieve a more general picture. Therefore, γ-ray DM searches should continue as a top priority for the DM community.

[10] Just before the submission of this article, a study of the DM annihilation in classical dSphs appeared [124]. Although using a different approach and methodology, the authors reach rather similar conclusions for those objects common to both studies, namely Ursa Minor and Draco. In particular, they also find that: i) substructures do not lead to important increments of the DM flux in dwarfs; ii) considering the angular extension of the sources is vital in order to plan the best search strategy; iii) assuming point-like emission from dSphs is indeed a very poor approximation for IACTs, and iv) sensitivities of present and future gamma-ray observatories seem to be quite far from detection.

[11] It seems that there is still room for further improvements of the present generation of IACTs, see e.g. Ref. [128].

Indeed, we are just now starting to really unveil the γ-ray energy window, and almost every month new sources are being discovered in the GeV–TeV sky. The time for γ-ray DM searches has definitely come.

Acknowledgments

We are truly grateful to Mike Kuhlen for useful discussions and comments on the implementation of the 3K10 substructure model. We also thank Beth Willman and Marla Geha for sharing their thoughts and concerns on Willman 1 and Segue 1. We greatly appreciate the help of Juan Betancort, Dan Coe, Michele Doro, Jorge Pérez-Prieto and Irene Puerto-Giménez. M.A.S.C. also acknowledges the hospitality of Universidad de Huelva, where part of this work was done. M. C. is a MultiDark fellow: the authors thank the support of the spanish MICINN Consolider-Ingenio 2010 Programme under grant MultiDark CSD2009-00064. M.E.G. and M.C. also acknowledge support from the project P07FQM02962 funded by "Junta de Andalucia", the Spanish MICINN-INFN(PG21) projects FPA2009-10773 and FPA2008-04063-E.

References

[1] G. Bertone, D. Hooper and J. Silk, *Particle dark matter: Evidence, candidates and constraints, Phys. Rept.* **405**, (2005) 279 [hep-ph/0404175].

[2] E. Komatsu *et al.* (WMAP Collaboration), *Seven-Year Wilkinson Microwave Anisotropy Probe (WMAP) Observations: Cosmological Interpretation, Astrophys. J. Suppl.* **192**, (2011) 18 [arXiv:1001.4538].

[3] F. D. Steffen, *Dark Matter Candidates - Axions, Neutralinos, Gravitinos, and Axinos, Eur. Phys. J.* C **59**, (2009) 557 [arXiv:0811.3347].

[4] M. A. Sánchez-Conde, D. Paneque, E. Bloom, F. Prada and A. Dominguez, *Hints of the existence of Axion-Like-Particles from the gamma-ray spectra of cosmological sources, Phys. Rev.* D **79**, (2009) 123511 [arXiv:0905.3270].

[5] G. Bertone, *Dark matter: The connection with gamma-ray astrophysics, Astrophys. Space Sci.* **309**, (2007) 505 [astro-ph/0608706].

[6] L. Bergstrom, *Dark matter candidates: A status report, AIP Conf. Proc.* **1241**, (2010) 49.

[7] J. A. Hinton (HESS Collaboration), *The status of the HESS project, New Astron. Rev.* **48**, (2004) 331 [astro-ph/0403052].

[8] E. Lorenz (MAGIC Collaboration), *Status of the 17-m MAGIC telescope, New Astron. Rev.* **48**, (2004) 339.

[9] T. C. Weekes, H. Badran, S. D. Biller *et al.*, *VERITAS: The Very energetic radiation imaging telescope array system, Astropart. Phys.* **17**, (2002) 221 [astro-ph/0108478].

[10] N. Gehrels, P. Michelson, *GLAST: The next generation high-energy gamma-ray astronomy mission, Astropart. Phys.* **11**, (1999) 277.

[11] F. Aharonian *et al.* (HESS Collaboration), *Very high-energy gamma rays from the direction of Sagittarius A*, Astron. Astrophys.* **425**, (2004) L13 [astro-ph/0408145].

[12] J. Albert *et al.* (MAGIC Collaboration), *Observation of gamma-rays from the galactic center with the magic telescope, Astrophys. J.* **638**, (2006) L101 [astro-ph/0512469].

[13] F. Aharonian *et al.* (HESS Collaboration), *H.E.S.S. observations of the Galactic Center region and their possible dark matter interpretation, Phys. Rev. Lett.* **97**, (2006) 221102 [astro-ph/0610509].

[14] N. W. Evans, F. Ferrer, S. Sarkar, *A 'Baedecker' for the dark matter annihilation signal, Phys. Rev.* D **69**, (2004) 123501 [astro-ph/0311145].

[15] L. E. Strigari, S. M. Koushiappas, J. S. Bullock *et al.*, *Precise constraints on the dark matter content of Milky Way dwarf galaxies for gamma-ray experiments, Phys. Rev.* D **75**, (2007) 083526 [astro-ph/0611925].

[16] A. Pinzke, C. Pfrommer, L. Bergstrom, *Gamma-rays from dark matter annihilations strongly constrain the substructure in halos, Phys. Rev. Lett.* **103**, (2009) 181302 [arXiv:0905.1948].

[17] D. Hooper, *TASI 2008 Lectures on Dark Matter,* [arXiv:0901.4090].

[18] J. Albert *et al.* (MAGIC Collaboration), *Upper limit for gamma-ray emission above 140-GeV from the dwarf spheroidal galaxy Draco, Astrophys. J.* **679**, (2008) 428 [arXiv:0711.2574].

[19] F. Aharonian (HESS Collaboration), *Observations of the Sagittarius Dwarf galaxy by the H.E.S.S. experiment and search for a Dark Matter signal, Astropart. Phys.* **29**, (2008) 55 [arXiv:0711.2369].

[20] M. Wood, G. Blaylock, S. M. Bradbury *et al.*, *A Search for Dark Matter Annihilation with the Whipple 10m Telescope, Astrophys. J.* **678**, (2008) 594 [arXiv:0801.1708].

[21] E. Aliu *et al.* (MAGIC Collaboration), *Upper limits on the VHE gamma-ray emission from the Willman 1 satellite galaxy with the MAGIC Telescope, Astrophys. J.* **697**, (2009) 1299 [arXiv:0810.3561].

[22] V. A. Acciari, *et al.* (VERITAS Collaboration), *VERITAS Search for VHE Gamma-ray Emission from Dwarf Spheroidal Galaxies, Astrophys. J.* **720**, (2010) 1174 [arXiv:1006.5955].

[23] F. Aharonian (HESS Collaboration), *A search for a dark matter annihilation signal towards the Canis Major overdensity with H.E.S.S, Astrophys. J.* **691**, (2009) 175 [arXiv:0809.3894].

[24] J. Aleksic *et al.* (MAGIC Collaboration), *Searches for Dark Matter annihilation signatures in the Segue 1 satellite galaxy with the MAGIC-I telescope, JCAP* **1106** (2011) 035. [arXiv:1103.0477].

[25] A. Abramowski *et al.* (HESS Collaboration), *H.E.S.S. constraints on Dark Matter annihilations towards the Sculptor and Carina Dwarf Galaxies, Astropart. Phys.* **34** (2011) 608. [arXiv:1012.5602].

[26] M. Kamionkowski, S. M. Koushiappas, M. Kuhlen, *Galactic Substructure and Dark Matter Annihilation in the Milky Way Halo, Phys. Rev.* D **81**, (2010) 043532 [arXiv:1001.3144].

[27] T. Bringmann, L. Bergstrom, J. Edsjo, *New Gamma-Ray Contributions to Supersymmetric Dark Matter Annihilation, J. High Energy Phys.* 01, (2008) 049 [arXiv:0710.3169].

[28] M. Cannoni, M. E. Gomez, M. A. Sánchez-Conde *et al.*, *Impact of internal bremsstrahlung on the detection of gamma-rays from neutralinos, Phys. Rev.* D **81**, (2010) 107303 [arXiv:1003.5164].

[29] M. Lattanzi, J. I. Silk, *Can the WIMP annihilation boost factor be boosted by the Sommerfeld enhancement?, Phys. Rev. D* **79**, (2009) 083523 [arXiv:0812.0360].

[30] L. Pieri, M. Lattanzi & J. Silk, *Constraining the dark matter annihilation cross-section with Cherenkov telescope observations of dwarf galaxies, Mon. Not. Roy. Astron. Soc.* **399** (2009), 2033

[31] A. Pinzke, C. Pfrommer & L. Bergstrom, *Prospects of detecting gamma-ray emission from galaxy clusters: cosmic rays and dark matter annihilations* (2011) [arXiv:1105.3240]

[32] R. Bernabei *et al.*, *New results from DAMA/LIBRA, Eur. Phys. J.* **C67**, (2010) 39 [arXiv:1002.1028 [astro-ph.GA]].

[33] C. E. Aalseth *et al.*, *Search for an Annual Modulation in a P-type Point Contact Germanium Dark Matter Detector* (2011) [arXiv:1106.0650 [astro-ph.CO]].

[34] M. Cannoni, *On the formalism and upper limits for spin-dependent cross sections in dark matter elastic scattering with nuclei* (2011) [arXiv:1108.4337 [hep-ph]].

[35] M. A. Pérez-Torres, F. Zandanel, M. A. Guerrero *et al.*, *The origin of the diffuse non-thermal X-ray and radio emission in the Ophiuchus cluster of galaxies, Mon. Not. Roy. Astron. Soc.* **396**, (2009) 2237 [arXiv:0812.3598].

[36] S. Colafrancesco, S. Profumo, P. Ullio, *Detecting dark matter WIMPs in the Draco dwarf: A multi-wavelength perspective, Phys. Rev.* D **75**, (2007) 023513 [astro-ph/0607073].

[37] S. Colafrancesco, P. Marchegiani, P. Giommi, *Disentangling the gamma-ray emission of NGC1275 and that of the Perseus cluster, Astron. Astrophys.* **519**, (2010) A82 [arXiv:1006.2333].

[38] G. Duda, G. Gelmini, P. Gondolo *et al.*, *Indirect detection of a subdominant density component of cold dark matter, Phys. Rev.* D **67**, (2003) 023505 [hep-ph/0209266].

[39] J. F. Navarro, C. S. Frenk, S. D. M. White, *The Structure of cold dark matter halos, Astrophys. J.* **462**, (1996) 563 [astro-ph/9508025].

[40] A. V. Kravtsov, A. A. Klypin, J. S. Bullock *et al.*, *The Cores of dark matter dominated galaxies: Theory versus observations, Astrophys. J.* **502**, (1998) 48 [astro-ph/9708176].

[41] J. F. Navarro, C. S. Frenk, S. D. M. White, *A Universal density profile from hierarchical clustering, Astrophys. J.* **490**, (1997) 493 [astro-ph/9611107].

[42] J. Diemand, M. Zemp, B. Moore *et al.*, *Cusps in CDM halos: The Density profile of a billion particle halo, Mon. Not. Roy. Astron. Soc.* **364**, (2005) 665 [astro-ph/0504215].

[43] J. Stadel, D. Potter, B. Moore *et al.*, *Quantifying the heart of darkness with GHALO - a multi-billion particle simulation of our galactic halo, Mon. Not. Roy. Astron. Soc.* **398**, (2009) L21 [arXiv:0808.2981].

[44] J. F. Navarro, A. Ludlow, V. Springel *et al.*, *The Diversity and Similarity of Cold Dark Matter Halos, Mon. Not. Roy. Astron. Soc.* **402**, (2010) 21 [arXiv:0810.1522].

[45] J. F. Navarro, E. Hayashi, C. Power *et al.*, *The Inner structure of Lambda-CDM halos 3: Universality and asymptotic slopes, Mon. Not. Roy. Astron. Soc.* **349**, (2004) 1039 [astro-ph/0311231].

[46] A. W. Graham, D. Merritt, B. Moore *et al.*, *Empirical models for Dark Matter Halos. I. Nonparametric Construction of Density Profiles and Comparison with Parametric Models, Astron. J.* **132**, (2006) 2685 [astro-ph/0509417].

[47] L. Gao, J. F. Navarro, S. Cole *et al.*, *The redshift dependence of the structure of massive LCDM halos, Mon. Not. Roy. Astron. Soc.* **387**, (2008) 536 [arXiv:0711.0746].

[48] F. Prada, A. Klypin, J. Flix Molina *et al.*, *Dark Matter Annihilation in the Milky Way Galaxy: Effects of Baryonic Compression, Phys. Rev. Lett.* **93**, (2004) 241301 [astro-ph/0401512].

[49] O. Y. Gnedin, J. R. Primack, *Dark Matter Profile in the Galactic Center, Phys. Rev. Lett.* **93**, (2004) 061302 [astro-ph/0308385].

[50] J. Diemand, P. Madau, B. Moore, *The Distribution and kinematics of early high-sigma peaks in present-day haloes: Implications for rare objects and old stellar populations, Mon. Not. Roy. Astron. Soc.* **364**, (2005) 367 [astro-ph/0506615].

[51] M. A. Sánchez-Conde, F. Prada, E. L. Lokas *et al.*, *Dark Matter annihilation in Draco: New considerations of the expected gamma flux, Phys. Rev.* D**76**, (2007) 123509 [astro-ph/0701426].

[52] D. J. H. Chung, L. L. Everett, G. L. Kane, S. F. King, J. D. Lykken and L. T. Wang, *The soft supersymmetry-breaking Lagrangian: Theory and applications, Phys. Rept.* **407**, (2005) 1 [hep-ph/0312378].

[53] D. Larson *et al.*, *Seven-Year Wilkinson Microwave Anisotropy Probe (WMAP) Observations: Power Spectra and WMAP-Derived Parameters, Astrophys. J. Suppl.* **192**, (2011) 16 [arXiv:1001.4635].

[54] Y. B. Zeldovich, A. A. Klypin, M. Y. Khlopov and V. M. Chechetkin, *Astrophysical Constraints On The Mass Of Heavy Stable Neutral Leptons, Sov. J. Nucl. Phys.* **31**, (1980) 664 [*Y*ad. Fiz. **31**, (1980) 1286]; J. Silk and M. Srednicki, *Cosmic-ray antiprotons as a probe of a photino-dominated universe, Phys. Rev. Lett.* **53**, (1984) 624; J. A. R. Cembranos, A. de la Cruz-Dombriz, A. Dobado, R. A. Lineros, A. L. Maroto, *Photon spectra from WIMP annihilation, Phys. Rev.* D **83** (2011) 083507 [arXiv:1009.4936 [hep-ph]].

[55] L. Bergstrom and P. Ullio, *Full one-loop calculation of neutralino annihilation into two photons, Nucl. Phys.* B **504**, (1997) 27 [hep-ph/9706232]; Z. Bern, P. Gondolo and M. Perelstein, *Neutralino annihilation into two photons, Phys. Lett.* B **411**, (1997) (1997) 86 [hep-ph/9706538]; P. Ullio and L. Bergstrom, *Neutralino annihilation into a photon and a Z boson, Phys. Rev.* D **57**, (1998) 1962 [hep-ph/9707333].

[56] L. Bergstrom, *Radiative processes in dark matter photini annihilation, Phys. Lett.* B **225**, (1989) 372; R. Flores, K. A. Olive and S. Rudaz, *Radiative processes in LSP annihilation, Phys. Lett.* B **232**, (1989) 377; L. Bergstrom, T. Bringmann, M. Eriksson and M. Gustafsson, *Gamma rays from heavy neutralino dark matter, Phys. Rev. Lett.* **95**, 241301 (2005) [hep-ph/0507229].

[57] P. Gondolo, J. Edsjo, P. Ullio, L. Bergstrom, M. Schelke and E. A. Baltz, *DarkSUSY: Computing supersymmetric dark matter properties numerically, J. Cosmol. Astropart. Phys.* 07, (2004) 008 [astro-ph/0406204]. http://www.darksusy.org .

[58] L. E. Strigari, J. S. Bullock, M. Kaplinghat *et al.*, *A common mass scale for satellite galaxies of the Milky Way, Nature* **454**, (2008) 1096-1097 [arXiv:0808.3772].

[59] V. Belokurov *et al.* (SDSS Collaboration), *Cats and Dogs, Hair and A Hero: A Quintet of New Milky Way Companions, Astrophys. J.* **654**, (2007) 897 [astro-ph/0608448].

[60] M. Geha, B. Willman, J. D. Simon *et al.*, *The Least Luminous Galaxy: Spectroscopy of the Milky Way Satellite Segue 1, Astrophys. J.* **692**, (2009) 1464 [arXiv:0809.2781].

[61] G. D. Martinez, J. S. Bullock, M. Kaplinghat *et al.*, *Indirect Dark Matter Detection from Dwarf Satellites: Joint Expectations from Astrophysics and Supersymmetry, J. Cosmol. Astropart. Phys.* 06, (2009) 014 [arXiv:0902.4715].

[62] M. Niederste-Ostholt, V. Belokurov, N. W. Evans *et al.*, *The Origin of Segue 1, Mon. Not. Roy. Astron. Soc.* **398**, (2009) 1771 [arXiv:0906.3669].

[63] G. D. Martinez, Q. E. Minor, J. Bullock *et al.*, *A Complete Spectroscopic Survey of the Milky Way satellite Segue 1: Dark matter content, stellar membership and binary properties from a Bayesian analysis, Astrophys. J.* **738**, (2011), 55 [arXiv:1008.4585].

[64] J. D. Simon, M. Geha, Q. E. Minor *et al.*, *A Complete Spectroscopic Survey of the Milky Way Satellite Segue 1: The Darkest Galaxy, Astrophys. J.* **733**, (2011), 46 [arXiv:1008.4585].

[65] B. Willman, M. Geha, J. Strader *et al.*, *Willman 1 - a probable dwarf galaxy with an irregular kinematic distribution, Astron. J.* **142**, (2011) 128 [arXiv:1007.3499].

[66] A. A. Abdo, *et al.* (Fermi-LAT Collaboration), *Observations of Milky Way Dwarf Spheroidal*

galaxies with the Fermi-LAT detector and constraints on Dark Matter models, Astrophys. J. **712**, (2010) 147 [arXiv:1001.4531].

[67] A. A. Abdo *et al.* (Fermi-LAT Collaboration), *The Spectrum of the Isotropic Diffuse Gamma-Ray Emission Derived From First-Year Fermi Large Area Telescope Data, Phys. Rev. Lett.* **104**, (2010) 101101 [arXiv:1002.3603].

[68] M. Mateo, *Dwarf galaxies of the Local Group, Ann. Rev. Astron. Astrophys.* **36**, (1998) 435 [astro-ph/9810070].

[69] A. Helmi, S. D. M. White, *Simple dynamical models of the Sagittarius dwarf galaxy, Mon. Not. Roy. Astron. Soc.* **323**, (2001) 529 [astro-ph/0002482].

[70] J. D. Simon, M. Geha, *The Kinematics of the Ultra-Faint Milky Way Satellites: Solving the Missing Satellite Problem, Astrophys. J.* **670**, (2007) 313 [arXiv:0706.0516].

[71] L. Pieri, A. Pizzella, E. M. Corsini *et al.*, *Could the Fermi-LAT detect gamma-rays from dark matter annihilation in the dwarf galaxies of the Local Group?, Astron. Astrophys.* **496**, (2009) 351 [arXiv:0812.1494].

[72] T. Bringmann, M. Doro, M. Fornasa, *Dark Matter signals from Draco and Willman 1: Prospects for MAGIC II and CTA, J. Cosmol. Astropart. Phys.* 01, (2009) 016 [arXiv:0809.2269].

[73] L. E. Strigari, S. M. Koushiappas, J. S. Bullock *et al.*, *The Most Dark-Matter-dominated Galaxies: Predicted Gamma-Ray Signals from the Faintest Milky Way Dwarfs, Astrophys. J.* **678**, (2008) 614 [arXiv:0706.0516]

[74] R. Essig,, N. Sehgal, L. E. Strigari, M. Geha, & J. D. Simon, Phys. Rev. D **82**, 123503 (2010) [arXiv:1007.4199].

[75] S. Kazantzidis, L. Mayer, C. Mastropietro *et al.*, *Density profiles of cold dark matter substructure: Implications for the missing satellites problem, Astrophys. J.* **608**, (2004) 663 [astro-ph/0312194].

[76] J. Binney & S. Tremaine, *Galactic Dynamics* (2008) (2nd ed.; Princeton, NJ: Princeton Univ. Press)

[77] N. Fornengo, L. Pieri, S. Scopel, *Neutralino annihilation into gamma-rays in the Milky Way and in external galaxies, Phys. Rev.* D **70**, (2004) 103529 [hep-ph/0407342].

[78] R. Essig, N. Sehgal, L. E. Strigari, M. Geha, J. D. Simon, *Indirect Dark Matter Detection Limits from the Ultra-Faint Milky Way Satellite Segue 1, Phys. Rev.* D**82** (2010) 123503 [arXiv:1007.4199].

[79] Peebles, P. J. E., *Priciples of physical cosmology,* (1993), Princeton Series in Physics, Princeton, NJ: Princeton University Press.

[80] G. M. Voit, *Tracing cosmic evolution with clusters of galaxies, Rev. Mod. Phys.* **77**, (2005) 207 [astro-ph/0410173].

[81] P. Blasi, S. Gabici, G. Brunetti, *Gamma rays from clusters of galaxies, Int. J. Mod. Phys.* A **22**, (2007) 681 [astro-ph/0701545].

[82] A. Pinzke, C. Pfrommer, *Simulating the gamma-ray emission from galaxy clusters: a universal cosmic ray spectrum and spatial distribution, Mon. Not. Roy. Astron. Soc.* **409**, (2010) 449 [arXiv:1001.5023].

[83] J. Aleksic *et al.* (MAGIC Collaboration), *MAGIC Gamma-Ray Telescope Observation of the Perseus Cluster of Galaxies: Implications for Cosmic Rays, Dark Matter and NGC 1275, Astrophys. J.* **710**, (2010) 634 [arXiv:0909.3267].

[84] F. A. Aharonian (HESS Collaboration), *Constraints on the multi-TeV particle population in the Coma Galaxy Cluster with H.E.S.S. observations, Astron. Astrophys.* **502**, (2009) 437

[arXiv:0907.0727].

[85] W. Domainko, D. Nedbal, J. A. Hinton *et al.*, *New results from H.E.S.S. observations of galaxy clusters, Int. J. Mod. Phys.* D **18**, (2009) 1627 [arXiv:0907.3001].

[86] F. Aharonian (HESS Collaboration), *Very high energy gamma-ray observations of the galaxy clusters Abell 496 and Abell 85 with H.E.S.S, Astron. Astrophys.* **495**, (2009) 27 [arXiv:0812.1638].

[87] J. S. Perkins *et al.* (Veritas Collaboration), *TeV gamma-ray observations of the perseus and abell 2029 galaxy clusters, Astrophys. J.* **644**, (2006) 148 [astro-ph/0602258].

[88] V. A. Acciari *et al.* (VERITAS Collaboration), *VERITAS observations of the BL Lac 1ES 1218+304, AIP Conf. Proc.* **1085**, (2009) 565 [arXiv:0901.4561].

[89] V. A. Acciari *et al.* (VERITAS Collaboration), *VERITAS Upper Limit on the VHE Emission from the Radio Galaxy NGC 1275, Astrophys. J.* **706**, (2009) L275 [arXiv:0911.0740].

[90] R. Kiuchi *et al.*, (CANGAROO Collaboration) *CANGAROO-III search for TeV Gamma-rays from two clusters of galaxies, Astrophys. J.* **704**, (2009) 240 [arXiv:0908.3301].

[91] O. Reimer, M. Pohl, P. Sreekumar *et al.*, *Egret upper limits on the high-energy gamma-ray emission of galaxy clusters, Astrophys. J.* **588**, (2003) 155 [astro-ph/0301362].

[92] M. Ackermann *et al.* (Fermi-LAT Collaboration), *GeV Gamma-ray Flux Upper Limits from Clusters of Galaxies, Astrophys. J.* **717**, (2010) L71 [arXiv:1006.0748].

[93] M. Ackermann, M. Ajello, A. Allafort *et al.*, *Constraints on Dark Matter Annihilation in Clusters of Galaxies with the Fermi Large Area Telescope, J. Cosmol. Astropart. Phys.* 05, (2010) 025 [arXiv:1002.2239].

[94] T. E. Jeltema, J. Kehayias, S. Profumo, *Gamma Rays from Clusters and Groups of Galaxies: Cosmic Rays versus Dark Matter, Phys. Rev.* D **80**, (2009) 023005 [arXiv:0812.0597].

[95] T. H. Reiprich, H. Böhringer, Astrophys. J. **567**, (2002) 716.

[96] P. Fouqué, J. M. Solanes, T. Sanchis *et al.*, *Structure, mass and distance of the virgo cluster from a tolman-bondi model, Astron. Astrophys.* **3755**, (2001) 770 [astro-ph/0106261].

[97] A. R. Duffy, J. Schaye, S. T. Kay *et al.*, *Dark matter halo concentrations in the WMAP5 cosmology, Mon. Not. Roy. Astron. Soc.* **390**, (2008) L64 [arXiv:0804.2486].

[98] N. Afshordi, R. Mohayaee, E. Bertschinger, *Hierarchy in the Phase Space and Dark Matter Astronomy, Phys. Rev.* D **81**, (2010) 101301 [arXiv:0911.0414].

[99] L. Pieri, G. Bertone, E. Branchini, *Dark Matter Annihilation in Substructures Revised, Mon. Not. Roy. Astron. Soc.* **384**, (2008) 1627 [arXiv:0706.2101].

[100] V. Springel, J. Wang, M. Vogelsberger *et al.*, *The Aquarius Project: the subhalos of galactic halos, Mon. Not. Roy. Astron. Soc.* **391**, (2008) 1685 [arXiv:0809.0898].

[101] M. Kuhlen, J. Diemand, P. Madau, *The Dark Matter Annihilation Signal from Galactic Substructure: Predictions for GLAST, Astrophys. J.* **686**, (2008) 262 [arXiv:0805.4416].

[102] S. Profumo, K. Sigurdson, M. Kamionkowski, *What mass are the smallest protohalos?, Phys. Rev. Lett.* **97**, (2006) 031301 [astro-ph/0603373].

[103] M. Kamionkowski, S. M. Koushiappas, *Galactic substructure and direct detection of dark matter, Phys. Rev.* D **77**, (2008) 103509 [arXiv:0801.3269].

[104] J. Diemand, M. Kuhlen, P. Madau *et al.*, *Clumps and streams in the local dark matter distribution, Nature* **454**, (2008) 735 [arXiv:0805.1244].

[105] L. Gao, C. S. Frenk, A. Jenkins, V. Springel & S. D. M.White, *Where will supersymmetric dark matter first be seen?, Mon. Not. Roy. Astron. Soc.* in press (2011) [arXiv:1107.1916]

[106] C. M. Urry, P. Padovani, *Unified schemes for radio-loud active galactic nuclei, Publ. Astron. Soc. Pac.* **107**, (1995) 803 [astro-ph/9506063].

[107] A. A. Abdo *et al.* (Fermi-LAT Collaboration), *Fermi Discovery of Gamma-Ray Emission from NGC 1275, Astrophys. J.* **699**, (2009) 31 [arXiv:0904.1904].

[108] C. Ferrari, F. Govoni, S. Schindler *et al.*, *Observations of extended radio emission in clusters, Space Sci. Rev.* **134**, (2008) 93 [arXiv:0801.0985].

[109] H. J. Volk, F. A. Aharonian, D. Breitschwerdt, *The nonthermal energy content and gamma-ray emission of starburst galaxies and clusters of galaxies, Space Sci. Rev.* **75**, (1996) 279.

[110] T. A. Ensslin, P. L. Biermann, P. P. Kronberg *et al.*, *Cosmic ray protons and magnetic fields in clusters of galaxies and their cosmological consequences, Astrophys. J.* **477**, (1997) 560 [astro-ph/9609190].

[111] C. Pfrommer, T. A. Ensslin, *Probing the cosmic ray population of the giant elliptical galaxy M 87 with observed TeV gamma-rays, Astron. Astrophys.* **407**, (2004) L73 [astro-ph/0306258].

[112] C. Pfrommer, T. A. Ensslin, *Constraining the population of cosmic ray protons in cooling flow clusters with gamma-ray and radio observations: Are Radio mini-halos of hadronic origin?, Astron. Astrophys.* **413**, (2004) 17 [astro-ph/0306257].

[113] C. Pfrommer, T. A. Ensslin, V. Springel *et al.*, *Simulating cosmic rays in clusters of galaxies. 1. Effects on the Sunyaev-Zel'dovich effect and the X-ray emission, Mon. Not. Roy. Astron. Soc.* **378**, (2007) 385 [astro-ph/0611037].

[114] C. Pfrommer, *Simulating cosmic rays in clusters of galaxies - III. Non-thermal scaling relations and comparison to observations, Mon. Not. Roy. Astron. Soc.* **385**, (2008) 1242 [arXiv:0707.1693].

[115] A. Loeb, E. Waxman, *Gamma-ray background from structure formation in the intergalactic medium, Nature* **405**, (2000) 156 [astro-ph/0003447].

[116] T. Totani, T. Kitayama, *Forming clusters of galaxies as the origin of unidentified GeV gamma-ray sources, Astrophys. J.* **545**, (2000) 572 [astro-ph/0006176].

[117] F. Miniati, *Inter-Galactic shock acceleration and the cosmic gamma-ray background, Mon. Not. Roy. Astron. Soc.* **337**, (2002) 199 [astro-ph/0203014].

[118] F. Miniati, *Numerical modeling of gamma radiation from galaxy clusters, Mon. Not. Roy. Astron. Soc.* **342**, (2003) 1009 [astro-ph/0303593].

[119] V. Petrosian, Y. Rephaeli, A. Bykov, *Nonthermal radiation mechanisms, Space Sci. Rev.* **134**, (2003) 191 [arXiv:0801.1016].

[120] CTA Consortium, *Design Concepts for the Cherenkov Telescope Array,* [arXiv:1008.3703].

[121] G. Brunetti, A. Lazarian, *Acceleration of primary and secondary particles in galaxy clusters by compressible MHD turbulence: from radio halos to gamma rays, Mon. Not. Roy. Astron. Soc.* **410**, (2011) 127 [arXiv:1008.0184].

[122] L. E. Strigari, S. M. Koushiappas, J. S. Bullock *et al.*, *The most dark-matter-dominated galaxies: predicted gamma-ray signals from the faintest Milky Way dwarfs, Astrophys. J.* **678**, (2008) 614 [astro-ph/0611925].

[123] MAGIC Collaboration, Crab performance paper, in preparation.

[124] A. Charbonnier, C. Combet, M. Daniel *et al.*, *Dark matter profiles and annihilation in dwarf spheroidal galaxies: prospectives for present and future gamma-ray observatories - I. The classical dSphs, Mon. Not. Roy. Astron. Soc.* accepted (2011) [arXiv:1104.0412].

[125] A. J. Cuesta, T. E. Jeltema, F. Zandanel *et al.*, *Dark Matter decay and annihilation in the*

Local Universe: CLUES from Fermi, Astrophys. J. Lett. **726**, (2011) L6 [arXiv:1007.3469].

[126] J. Ke, M. Luo, L. Wang *et al.*, *Gamma-rays from Nearby Clusters: Constraints on Selected Decaying Dark Matter Models, Phys. Lett.* B **698**, (2011) 44 [arXiv:1101.5878].

[127] J. Buckley, E. A. Baltz, G. Bertone *et al.*, *Section on Prospects for Dark Matter Detection of the White Paper on the Status and Future of Ground-Based TeV Gamma-Ray Astronomy,* [arXiv:0812.0795].

[128] Y. Becherini, A. Djannati-Ataï, V. Marandon, M. Punch & S. Pita, *A new analysis strategy for detection of faint ?-ray sources with Imaging Atmospheric Cherenkov Telescopes* Astroparticle Physics, **34**, (2011) 858 [arXiv:1104.5359].